blood®
Regular Article

Check for updates

MYELOID NEOPLASIA

HMGA1 chromatin regulators induce transcriptional networks involved in GATA2 and proliferation during MPN progression

Liping Li,[1,*] Jung-Hyun Kim,[1,*] Wenyan Lu,[1] Donna M. Williams,[1] Joseph Kim,[1] Leslie Cope,[2] Raajit K. Rampal,[3] Richard P. Koche,[3] Lingling Xian,[1] Li Z. Luo,[1] Marija Vasiljevic,[1] Daniel R. Matson,[4] Zhizhuang Joe Zhao,[5] Ophelia Rogers,[1] Matthew C. Stubbs,[6] Karen Reddy,[7] Antonio-Rodriguez Romero,[8] Bethan Psaila,[8] Jerry L. Spivak,[1,2] Alison R. Moliterno,[1] and Linda M. S. Resar[1,2,9,10]

[1]Division of Hematology, Department of Medicine, and [2]Department of Oncology, The Johns Hopkins University School of Medicine, Baltimore, MD; [3]Human Oncology and Pathogenesis Program, Leukemia Service, Department of Medicine, Center for Epigenetics Research, Memorial Sloan Kettering Cancer Institute, New York, NY; [4]Blood Cancer Research Institute, Department of Cell and Regenerative Biology, UW Carbone Cancer Center, University of Wisconsin School of Medicine, Madison, WI; [5]Department of Pathology, University of Oklahoma Health Sciences Center, Oklahoma City, OK; [6]Pharmacology, Incyte Research Institute, Wilmington, DE; [7]Department of Biologic Chemistry, The Johns Hopkins University School of Medicine, Baltimore, MD; [8]MRC Weatherall Institute of Molecular Medicine, Radcliffe Department of Medicine and National Institutes of Health Research (NIHR) Oxford Biomedical Research Centre, University of Oxford, Oxford, UK; and [9]Cellular and Molecular Medicine Graduate Program and [10]Department of Pathology, The Johns Hopkins University School of Medicine, Baltimore, MD

KEY POINTS

- **HMGA1 is a novel epigenetic switch that induces aberrant transcriptional networks during MPN progression to MF and AML.**
- **HMGA1 deficiency prevents MF and enhances sensitivity to ruxolitinib, prolonging survival in murine models of *JAK2*^{V617F} AML.**

Myeloproliferative neoplasms (MPNs) transform to myelofibrosis (MF) and highly lethal acute myeloid leukemia (AML), although the actionable mechanisms driving progression remain elusive. Here, we elucidate the role of the high mobility group A1 (HMGA1) chromatin regulator as a novel driver of MPN progression. *HMGA1* is upregulated in MPN, with highest levels after transformation to MF or AML. To define HMGA1 function, we disrupted gene expression via CRISPR/Cas9, short hairpin RNA, or genetic deletion in MPN models. HMGA1 depletion in *JAK2*^{V617F} AML cell lines disrupts proliferation, clonogenicity, and leukemic engraftment. Surprisingly, loss of just a single *Hmga1* allele prevents progression to MF in *JAK2*^{V617F} mice, decreasing erythrocytosis, thrombocytosis, megakaryocyte hyperplasia, and expansion of stem and progenitors, while preventing splenomegaly and fibrosis within the spleen and BM. RNA-sequencing and chromatin immunoprecipitation sequencing revealed HMGA1 transcriptional networks and chromatin occupancy at genes that govern proliferation (E2F, G2M, mitotic spindle) and cell fate, including the *GATA2* master regulatory gene. Silencing *GATA2* recapitulates most phenotypes observed with HMGA1 depletion, whereas *GATA2* re-expression partially rescues leukemogenesis. HMGA1 transactivates *GATA2* through sequences near the developmental enhancer (+9.5), increasing chromatin accessibility and recruiting active histone marks. Further, HMGA1 transcriptional networks, including proliferation pathways and *GATA2*, are activated in human MF and MPN leukemic transformation. Importantly, HMGA1 depletion enhances responses to the JAK2 inhibitor, ruxolitinib, preventing MF and prolonging survival in murine models of *JAK2*^{V617F} AML. These findings illuminate HMGA1 as a key epigenetic switch involved in MPN transformation and a promising therapeutic target to treat or prevent disease progression.

Introduction

Myeloproliferative neoplasms (MPNs) are clonal hematopoietic stem cell (HSC) disorders that are characterized by hyperactive JAK/STAT signaling and an increased risk for transformation to myelofibrosis (MF) and acute myeloid leukemia (AML).[1-18] However, actionable mechanisms driving progression remain elusive, and therapies are ineffective after leukemic transformation. The most common driver mutation, *JAK2*^{V617F}, enhances phosphorylation of STAT3/5 proteins, leading to overproduction of myeloid lineages.[19-22] Most patients present with chronic indolent disease and elevations in platelets (essential thrombocythemia; ET) or red cells and platelets (polycythemia vera; PV), although a subset presents with primary MF that is characterized by bone marrow (BM) and splenic fibrosis, osteosclerosis, splenomegaly, pancytopenia, and shortened life spans.[1-22] Although transformation to MF or AML is associated with acquisition of new mutations, therapies to prevent or treat transformation are lacking.[2-26]

Chromatin regulators maintain gene expression, conferring plasticity and other stem cell properties during development and

Downloaded from http://ashpublications.org/blood/article-pdf/139/18/2797/1895455/bloodbld2021013925.pdf by guest on 29 September 2023

oncogenic transformation.[27] The *HMGA1* chromatin regulator gene is highly expressed in embryonic and adult stem cells, with low or undetectable levels in most differentiated tissues.[28-33] In diverse solid tumors, *HMGA1* is aberrantly re-expressed; high levels are associated with adverse outcomes.[28-30,33-44] Located on chromosome 6p21, *HMGA1* encodes HMGA1a/HMGA1b protein isoforms that bind to AT-rich regions in DNA, displacing repressive histones that compact chromatin.[28,29,34,45-52] After binding DNA and "opening" the minor groove, HMGA1 recruits transcriptional complexes to modulate gene expression.[28,29,34,45-52] Transgenic mice overexpressing *Hmga1* in lymphoid cells develop clonal expansion and leukemia.[53-56] *HMGA1* is also overexpressed in human lymphoid and myeloid malignancies.[53-61] Intriguingly, a recent study found that germline lesions within the *HMGA1* loci predispose individuals to MPN.[62] However, the role of HMGA1 in MPN had not been elucidated.

Here, we report that HMGA1 is upregulated and activates specific transcriptional networks during MPN progression. HMGA1 deficiency enhances sensitivity to the JAK inhibitor ruxolitinib and delays leukemogenesis in murine models of *JAK2*^{V617} AML. Further, deletion of just a single *Hmga1* allele prevents MF in *JAK2*^{V617F} mice. Our findings demonstrate that HMGA1 is a key epigenetic switch in MPN, thus opening the door to novel therapeutic approaches to treat or prevent progression.

Methods

Murine models

Hmga1-deficient mice[44,63] and *JAK2*^{V617F} transgenic mice[64,65] were crossed to obtain the desired genotypes. We generated leukemia xenografts (DAMI/SET-2 cells; 1-5 $\times$ 10^6) by tail vein injection into NOD Scid γ (NSG) mice. For transplantation studies, BM cells (4 $\times$ 10^6) from 16-week donors (*JAK2*$^{V617F/V617F}$ vs *JAK2*$^{V617F/V617F}$ with *Hmga1* heterozygosity [*Hmga1*$^{+/-}$]) were injected into lethally irradiated recipients (8 weeks; Ly5.1, 10 Gy).

Patient samples, cell lines, and in vitro studies

Patient samples, protein and RNA analyses, chromatin immunoprecipitation sequencing (ChIPseq), chromatin immunoprecipitation polymerase chain reaction (ChIP-PCR), assay for transposase-accessible chromatin-sequencing (ATACseq), flow cytometry, immunohistochemistry, and cell-based assays were performed as described.[31-33,40-44,53-61,66-72] RNA sequencing (RNAseq)/ATACseq and ChIP-PCR in parental DAMI cells (with and without *HMGA1* silencing) were performed in triplicate. DAMI (American Type Culture Collection),[73,74] SET-2 (Leibniz Institute DSMZ),[75] and UKE-1 (Coriell Institute)[76] were cultured as recommended.

RNAseq analysis

RNAseq of *JAK2*^{V617F} AML cells (DAMI/SET-2) was performed after transduction with control lentivirus or short hairpin RNA (shRNA) targeting *HMGA1*. Following data analyses, pathways were identified via MSig gene set enrichment analysis (GSEA).[77,78] Data from RNAseq, Gene Expression Omnibus data sets (GSE103237,[79] GSE122198,[71] GSE144568[70]), and peripheral blood mononuclear cells (PBMCs) from matched patients with MF that transformed to AML were analyzed as described.[26]

Single-cell RNAseq (scRNAseq) was performed in BM-derived lineage$^-$sca1$^+$c-kit$^+$ (LSK) cells from *JAK2*$^{V617F/V617F}$ mice with both *Hmga1* alleles intact or with *Hmga1* heterozygous deficiency (2 mice per condition) and analyzed as described.[71,72]

Statistical analysis

After ascertaining normal distributions (Ryan-Joyner, D'Agostino-Pearson tests), data were analyzed with a 2-tailed Student *t* test for 2 groups or 1-way analysis of variance (ANOVA), followed by Tukey's multiple-comparison test; if not normal, we used the Mann-Whitney *U* test for 2 groups and the Kruskal-Wallis test, followed by Dunn's test, for multiple comparisons. Cytotoxicity curves were analyzed by 2-way ANOVA. We compared survival using the Kaplan-Meier test, with the log-rank (Mantel-Cox) test and the Bonferroni method for multiple comparisons. Fisher's exact test was used to compare differences in scRNAseq clusters across genotype. $P < .05$ was considered significant (GraphPad Prism 8.)

Additional details about methods and RNAseq analyses are provided in supplemental Methods (available on the *Blood* Web site).

Results

HMGA1 is overexpressed in MPN progression

To explore *HMGA1* function in MPN, we first assessed gene expression in CD34$^+$ cells from patients with MPN with acquired *JAK2*^{V617F} mutations (Figure 1A). Compared with unaffected individuals, *HMGA1* was upregulated in peripheral blood (PB) CD34$^+$ cells, with the highest levels after leukemic transformation. In a separate cohort (GSE103237),[79] *HMGA1* was overexpressed in BM CD34$^+$ cells from *JAK2*^{V617F} ET and PV. Intriguingly, *HMGA1* was not overexpressed in *CALR*-mutant ET. By scRNAseq of PB CD34$^+$ cells (GSE122198),[71] *HMGA1* was also overexpressed in *JAK2*^{V617F} mutant cells from MF compared with unmutated cells from the same patients or unaffected individuals. *HMGA1* overexpression in CD34$^+$ cells from patients with MF compared with age-matched healthy individuals was confirmed by scRNAseq in another cohort (GSE144568[70]). Together, these data demonstrate that *HMGA1* is upregulated in *JAK2*^{V617} MPNs.

HMGA1 is required for proliferation, clonogenicity, and leukemic engraftment

Next, we disrupted gene expression via shRNA targeting 2 *HMGA1* sequences or by CRISPR/Cas9 in *JAK2*^{V617F} AML cell lines (DAMI, SET-2, UKE-1).[73-76] Strikingly, depleting *HMGA1* in all cell lines disrupts proliferation and clonogenicity, decreasing colony number and size (Figure 1B-D; supplemental Figure 1A-F). *HMGA1* depletion also decreases the percentage of cells in S phase while increasing apoptosis (Figure 1E-F). Notably, HMGA2, a related HMGA family member, did not change with *HMGA1* silencing (supplemental Figure 1A). Next, we compared leukemic engraftment following tail vein injection of AML cells into NSG mice. HMGA1 depletion in DAMI or SET-2 cells decreases spleen size, circulating blasts, and leukemic engraftment in BM and spleen 23 days following injection (Figure 1G-H; supplemental Figure 2A). BM architecture was generally normal in recipients of HMGA1-depleted cells, whereas architecture was effaced by leukemic blasts in recipients of AML cells

Downloaded from http://ashpublications.org/blood/article-pdf/139/18/2797/1895455/bloodbld2021013925.pdf by guest on 29 September 2023

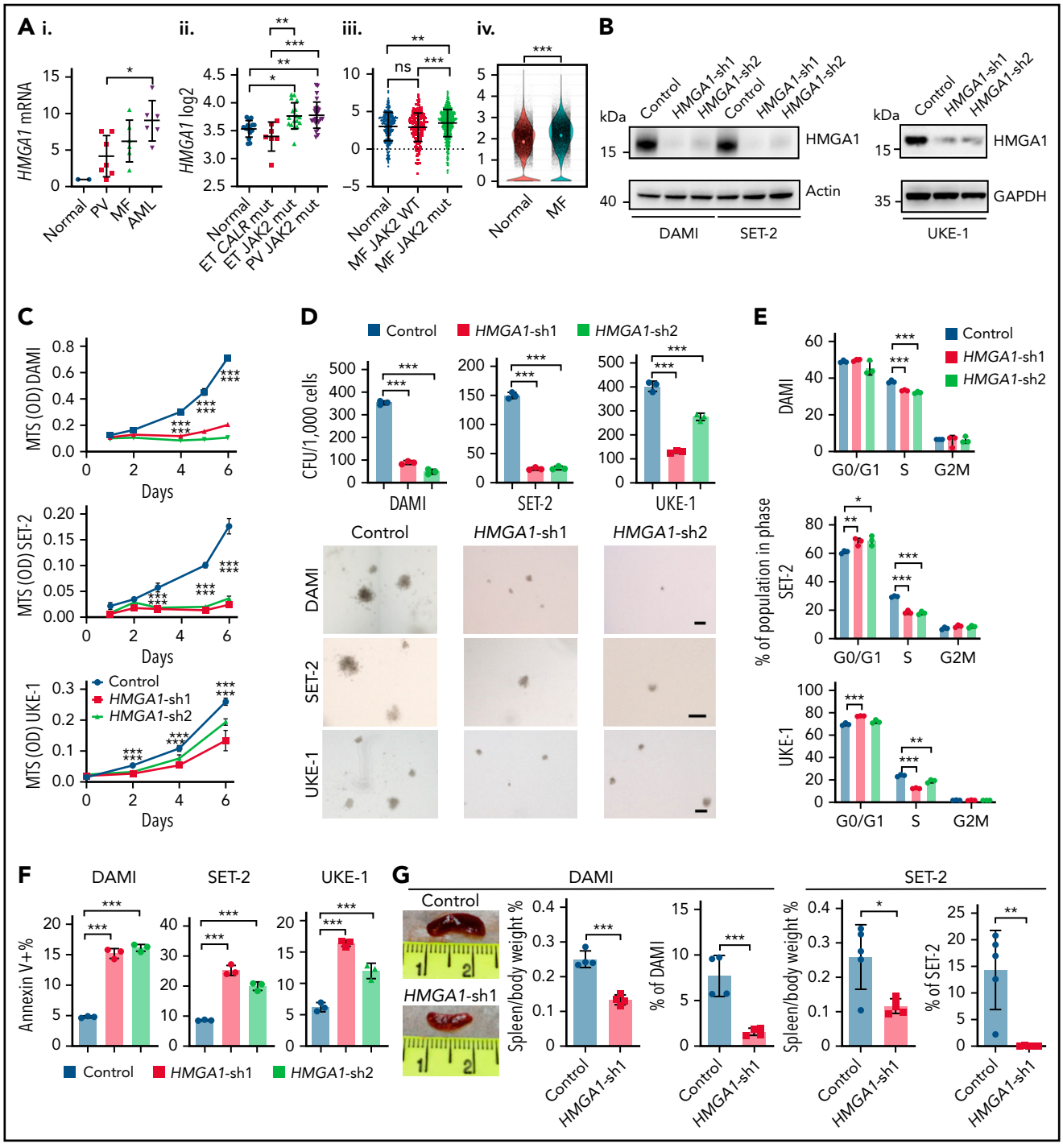

Figure 1. *HMGA1* is upregulated during MPN progression and required for leukemia engraftment. (Ai) Relative *HMGA1* expression (mean ± standard deviation [SD]) performed in triplicate (quantitative polymerase chain reaction) in $CD34^+$ cells from patients with MPN with acquired $JAK2^{V617F}$ mutations (PV, n = 8; MF, n = 5; AML, n = 6) or control subjects (Normal; n = 2). *RPLP0* was used to control for loading. $^*P < .05$, 1-way ANOVA, followed by Tukey's multiple-comparison test. (Aii) *HMGA1* expression in $CD34^+$ cells from BM of patients with MPN with $JAK2^{V617F}$ ET (n = 17), $JAK2^{V617F}$ PV (n = 26), or *CALR*-mutant ET (n = 7) or from unaffected individuals (n = 15) by microarray. Each point represents a single patient. $^*P < .05$, $^{**}P < .01$, $^{***}P < .001$, 1-way ANOVA, followed by Tukey's multiple-comparison test. (Aiii) *HMGA1* expression in *JAK2*-mutant $CD34^+$ PB cells from patients with MF compared with unmutated $CD34^+$ cells from the same patient with MF (n = 8) and unaffected individuals (n = 2) by scRNAseq; each point represents the expression level for a single cell. $^{**}P < .01$, $^{***}P < .001$, 1-way ANOVA, followed by Tukey's multiple-comparison test. (Aiv) *HMGA1* expression in lineage$^-$ $CD34^+$ PB from patients with MF and age-matched healthy donors. *HMGA1* was detected in 81.1% of cells (30 786/37 941) from healthy donors and in 89.7% of cells (34 038/37 941) from patients with MF. White dots on the violin plot indicate the mean level of expression; black points represent expression values for each single cell. $^{***}P \leq .001$, Wilcoxon rank-sum test. (B) Western blot analysis of HMGA1, β-actin, and GAPDH (loading control) protein levels from DAMI, SET-2, and UKE-1 cells, with or without *HMGA1* silencing. Western blots were performed 3 times; a representative blot is shown. Size markers (kDa) are indicated. (C) Proliferation (mean ± SD) estimated by MTS [3-(4,5-dimethylthiazol-2-yl)-5-(3-carboxymethoxyphenyl)-2-(4-sulfophenyl)-2H-tetrazolium; Promega)] in DAMI, SET-2, and UKE-1 cells, with or without *HMGA1* silencing (control vs *HMGA1*-sh1 or *HMGA1*-sh2; mean ± SD, at the indicated time points. $^{***}P < .001$, 2-tailed Student *t* test. (D) Colony-forming units (CFU; mean ± SD) in DAMI, SET-2, and UKE-1 cells, with or without *HMGA1* silencing (control vs *HMGA1*-sh1 or *HMGA1*-sh2), performed in triplicate from 2 independent experiments (upper panels). Representative images of colonies are shown (lower panels). Scale bars,

Downloaded from http://ashpublications.org/blood/article-pdf/139/18/2797/1895455/bloodbld2021013925.pdf by guest on 29 September 2023

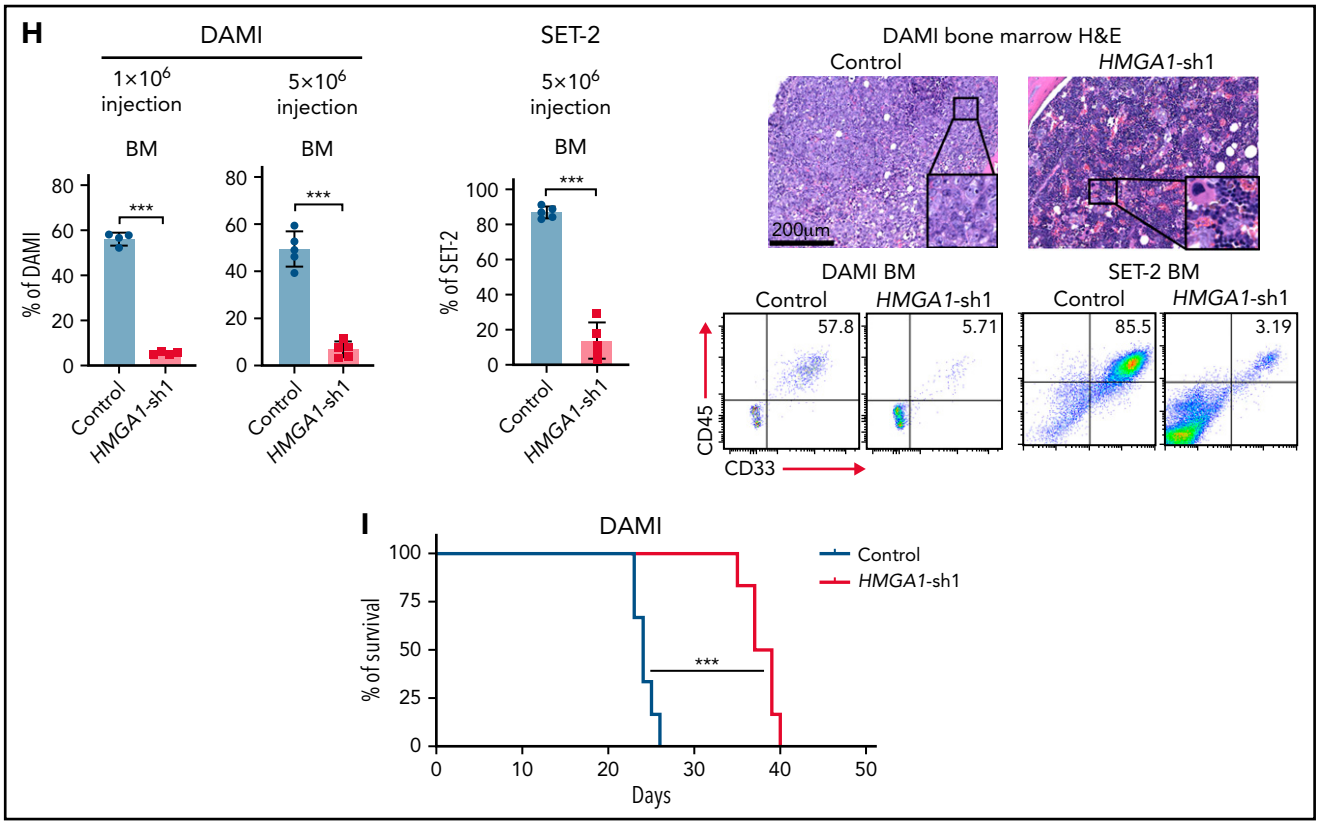

Figure 1 (continued) 200 μm. ***$P < .001$; 2-tailed Student *t* test. (E) Edu (5-ethynyl-2′-deoxyuridine) cell cycle analysis (mean ± SD) by flow cytometry assessed in DAMI, SET-2 and UKE-1 cells, with or without *HMGA1* silencing (control vs *HMGA1*-sh1 or *HMGA1*-sh2), performed in triplicate from 2 independent experiments; *$P < .05$, **$P < .01$, ***$P < .001$; 2-tailed Student *t* test. (F) Annexin V apoptosis by flow cytometry assessed in DAMI, SET-2, and UKE-1 cells, with or without *HMGA1* silencing (control vs *HMGA1*-sh1 or *HMGA1*-sh2), performed in triplicate from 2 independent experiments, ***$P < .001$; 2-tailed Student *t* test. Representative density plots from each group are also shown. (G) Representative images of spleens and graphical comparisons of relative spleen weight (spleen/body weight %; mean ± SD); leukemia cell engraftment by flow cytometry (mean ± SD) in spleen from NSG mice injected with DAMI cells and SET-2 cells, with or without *HMGA1* silencing (control vs *HMGA1*-sh1; n = 4 or 5 per group). *$P < .05$, **$P < .01$, ***$P < .001$; 2-tailed Student *t* test. (H) Leukemia cell engraftment (mean ± SD) assessed by flow cytometry in BM from NSG mice injected with DAMI cells (left panel) or SET-2 cells (middle panel), with or without *HMGA1* silencing (control vs *HMGA1*-sh1; n = 4 or 5 per group). Representative flow cytometry plots from each group and hematoxylin and eosin-stained BM from DAMI cells (right panels). Scale bar, 200 μm. ***$P < .001$; 2-tailed Student *t* test. (I) Survival analysis by Kaplan-Meier estimate in NSG mice injected with DAMI cells, with or without *HMGA1* silencing (Control: median survival, 24 days vs *HMGA1*-sh1: median survival, 38 days; n = 6 per group). ***$P < .001$, log-rank (Mantel-Cox) test. mRNA, messenger RNA; ns, not significant.

lacking HMGA1 depletion. Survival was also prolonged in recipients of AML cells with *HMGA1* silencing (Figure 1I; supplemental Figure 2A). Intriguingly, the small percentage of engrafted blasts from the pool of AML cells with *HMGA1* silencing express higher *HMGA1* than do the injected cells, suggesting that escape from gene silencing allows these cells to engraft (supplemental Figure 2B-C). Our findings indicate that HMGA1 is required for salient AML phenotypes, including proliferation, clonogenicity, and leukemic engraftment.

Hmga1 haploinsufficiency prevents progression to MF

To investigate HMGA1 in models of chronic MPN, we crossed a well-characterized *JAK2*^{V617F} transgenic model[64,65] onto a background with global heterozygous *Hmga1* deficiency.[44,63] *JAK2*^{V617F} mice express 13 copies of the transgene and recapitulate features of chronic MPN with erythrocytosis and thrombocytosis by 12 weeks and progression to MF by 40 weeks, with osteosclerosis, splenomegaly, and fibrosis involving the spleen and BM (Figure 2; supplemental Figure 3A). Importantly, *Hmga1* heterozygous mice have normal life spans and unperturbed hematopoiesis, based on steady-state blood counts, for up to 60 weeks (supplemental Figure 3B). Strikingly, loss of a single *Hmga1* allele in *JAK2*^{V617F} mice prevents progression to MF, decreasing erythrocytosis by 12 weeks, and thrombocytosis, megakaryocyte hyperplasia, splenomegaly, fibrosis (spleen, BM) and osteosclerosis after 40 weeks (Figure 2).

To determine whether these effects depend on *Hmga1* within the hematopoietic compartment, we transplanted BM from mice biallelic for the *JAK2*^{V617F} transgene (26 copies; denoted *JAK2*$^{V617F/V617F}$) with *Hmga1* heterozygosity or both alleles intact into lethally irradiated recipients. As before, *Hmga1* deficiency decreased erythrocytosis, thrombocytosis, megakaryocyte hyperplasia, splenomegaly, and fibrosis (spleen, BM) (Figure 3A-D), demonstrating that *Hmga1* haploinsufficiency within hematopoietic cells is responsible for abrogating MF.

Hmga1 haploinsufficiency dampens expansion of *JAK*$^{V617F/V617F}$ HSCs and progenitors

To determine how Hmga1 prevents MF, we assessed the frequency and function of hematopoietic stem cells (HSCs) and

Downloaded from http://ashpublications.org/blood/article-pdf/139/18/2797/1895455/bloodbld2021013925.pdf by guest on 29 September 2023

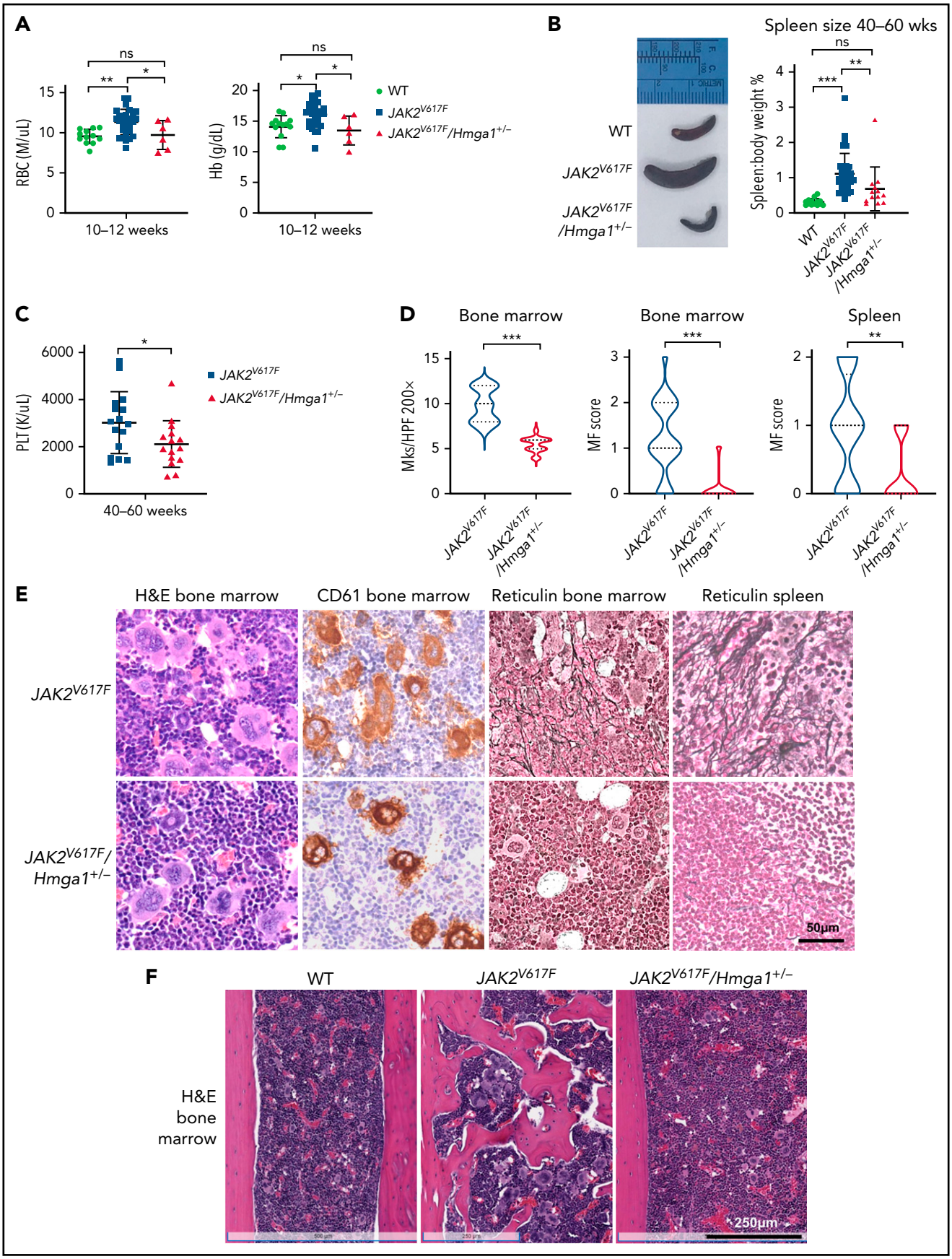

Figure 2.

Downloaded from http://ashpublications.org/blood/article-pdf/139/18/2797/1895455/bloodbld2021013925.pdf by guest on 29 September 2023

hematopoietic stem and progenitor cells (HSPCs). Long-term HSCs, LSK cells, and myeloid progenitors, including multipotent progenitors, granulocyte-monocyte progenitors (GMPs), and megakaryocyte-erythrocyte progenitors (MEPs) all decrease in BM from $JAK^{V617F/V617F}$ transplants with *Hmga1* haploinsufficiency. LSK cells, multipotent progenitors, common myeloid progenitors, GMPs, and MEPs decrease in spleen (Figure 3E), although there was no difference in common lymphoid progenitors (CLPs) in marrow or spleen (supplemental Figure 4). *Hmga1* heterozygosity also dampens the clonogenic potential of $JAK2^{V617F/V617F}$ BM and spleen cells, decreasing total colony-forming units, granulocyte-monocyte colony-forming units, and burst-forming unit-erythroid (supplemental Figure 5). These data demonstrate that *Hmga1* haploinsufficiency within $JAK^{V617F/V617F}$ HSCs dampens clonogenicity and expansion in HSCs and distinct progenitors.

To further characterize HSPCs regulated by *Hmga1*, we compared scRNAseq in BM-derived LSK cells from $JAK2^{V617F/V617F}$ mice and $JAK2^{V617F/JAKV617F}$ mice with *Hmga1* heterozygous deficiency. Cell identify was assigned to clusters using published results.[72,80-83] Similar to our flow cytometry results, the cluster(s) enriched for markers of HSCs (cluster 7), megakaryocyte-biased progenitors (cluster 8), and megakaryocyte/erythroid-biased progenitors (clusters 5-6) all decreased in $JAK2^{V617F}$ mice with *Hmga1* heterozygous deficiency, whereas those with lymphoid-biased progenitor markers (clusters 0-1) increased (Figure 3F). These findings parallel our flow cytometry results, demonstrating that *Hmga1* deficiency mitigates expansion in HSCs and distinct progenitors involved in MPN.

HMGA1 activates transcriptional networks involved in proliferation and cell fate

To further elucidate the molecular underpinnings of HMGA1, we performed RNAseq in DAMI and SET-2 cells and ChIPseq/ATACseq in DAMI cells. GSEA from RNAseq revealed an HMGA1 signature of genes involved in cell cycle progression (E2F targets, G2M checkpoint, mitotic spindle, MYC targets) and cell fate decisions (GATA2 transcriptional networks; Figure 4A-C). Ingenuity Pathway Analysis showed similar networks, in addition to those governing cell-cell signaling, inflammation, and fibrosis. To determine which genes could be direct targets of HMGA1, we integrated RNAseq with ChIPseq to detect differentially regulated genes with HMGA1 occupancy in potential gene-regulatory regions, which identified E2F targets, mitotic spindle, G2M checkpoint, and GATA2 networks (supplemental Table 1). ATACseq showed differentially enhanced chromatin accessibility in DAMI control cells compared with cells with HMGA1 depletion in promoters for genes regulating cell growth and signal transduction. Integrating RNAseq/ATACseq (by Enrichr; supplemental Table 2) revealed enrichment for GATA genes, KRAS signaling, and active histone marks H3 lysine 4 monomethylation (H3K4me1) or H3 lysine 4 trimethylation (H3K4me3). We focused on *GATA2*, given its robust regulation by HMGA1 in $JAK2^{V617F}$ AML cells, role in HSC fate, and association with poor outcomes in myeloid malignancies.[84-87] HMGA1-dependent expression of *GATA2* was validated (messenger RNA, protein) in DAMI, SET-2, and UKE-1 cells with *HMGA1* deficiency via *HMGA1* shRNA or CRISPR/Cas9 (Figure 4D-E; supplemental Figure 6A-B). Conversely, *HMGA1* overexpression via CRISPR activation (*HMGA1*-CRISPRa) upregulates *GATA2* (supplemental Figure 6C).

HMGA1 and *GATA2* are coexpressed in HSPCs

Next, we determined whether *HMGA1* and *GATA2* are coexpressed in wild-type (WT) or $JAK2^{V617F}$-mutant HSPCs. In unaffected human and murine HSPCs, *HMGA1/Hmga1* and *GATA2/Gata2* are positively correlated (supplemental Figure 6D-G). In $JAK2^{V617F}$ murine HSPCs, *Hmga1* and *Gata2* are coexpressed and positively correlated, but only in LSK cells and MEPs (no correlation in common myeloid progenitors or GMPs; supplemental Figure 6H-I). Notably, LSK cell and MEP populations constitute MPN progenitors in $JAK2^{V617F}$ models.[88] These findings demonstrate coexpression of *HMGA1* and *GATA2* in HSPCs and MPN progenitors in $JAK2^{V617F}$ mice.

HMGA1 induces *GATA2* by binding to the developmental enhancer, increasing chromatin accessibility, and recruiting active histone marks

To determine whether HMGA1 directly activates *GATA2*, we identified 42 putative DNA binding sites throughout *GATA2* regulatory regions using in silico algorithms, including 6 regions with ≥2 sites within 500 bp. HMGA1 chromatin occupancy at these 6 regions by ChIP-PCR and ChIPseq show the greatest enrichment around an established +9.5 *GATA2* enhancer (Figure 4F-H) that is critical for HSC and MEP development during embryonic hematopoiesis.[84-86] Further, HMGA1 occupancy (ChIP-PCR) was depleted by *HMGA1* silencing (Figure 4F-I). This +9.5 enhancer partially overlaps with a 224-bp sequence with 4 predicted HMGA1 binding sites (A, B, C, D). ChIP-PCR, used to compare occupancy around these sites, showed the greatest enrichment at sites A and B; recombinant HMGA1 binding by gel shift analysis was also most robust with probes within site A or B (Figure 4H-J; supplemental Figure 7A-E). Because HMGA1 induces *GATA2* and associates with regions with active histone marks by ATACseq (H3K4me1, H3K4me3), we compared these marks by ChIP-PCR, which revealed enrichment at the +9.5 enhancer; both decreased upon *HMGA1* depletion (Figure 4H-I). Conversely, there was no change in H3K27Ac or control histone H3 binding, suggesting that HMGA1 recruits H3K4me1/H3K4me3 in $JAK2^{V617F}$ AML DAMI cells (supplemental Figure 7F-G).

To determine whether HMGA1 transactivates the *GATA2* developmental enhancer, we assessed luciferase reporter gene

Figure 2. *Hmga1* is required for progression of chronic MPN to MF in JAK^{V617F}-mutant mice. (A) Red blood cell (RBC) count and hemoglobin (Hb) (mean ± standard deviation [SD]) in PB from 10- to 12-week-old WT, $JAK2^{V617F}$, and $JAK2^{V617F}/Hmga1^{+/-}$ mice. (B) Representative spleens (left panel) and graph showing relative spleen sizes (right panel; mean ± SD) in WT, $JAK2^{V617F}$, and $JAK2^{V617F}/Hmga1^{+/-}$ mice. (C) Platelet (PLT) count from 40- to 60-week-old $JAK2^{V617F}$ and $JAK2^{V617F}/Hmga1^{+/-}$ mice. (D) Megakaryocytes per high-power field (Mks/HPF) in BM from $JAK2^{V617F}$ and $JAK2^{V617F}/Hmga1^{+/-}$ mice (left panel). MF scores in BM (middle panel) and spleen (right panel) from $JAK2^{V617F}$ and $JAK2^{V617F}/Hmga1^{+/-}$ mice. (E) Representative images from mouse models stained with hematoxylin and eosin (H&E of BM from femurs; left panels), CD61 by immunohistochemistry (BM from femurs; left middle panels), fibrosis (BM reticulin stain; right middle panels) and splenic fibrosis (reticulin; right panels)). Scale bar, 50 μm. (F) Representative images of BM from the femurs of WT, $JAK2^{V617F}$, and $JAK2^{V617F}/Hmga1^{+/-}$ mice (H&E stain). Scale bars, 250 μm. Data in (A-D) are mean ± standard deviation. $^*P < .05$, $^{**}P < .01$, $^{***}P < .001$, 1-way ANOVA, followed by Tukey's multiple-comparison test (A [right panel]), Kruskal-Wallis test, followed by Dunn's multiple-comparison test (A [left panel], B), Mann-Whitney *U* test (C), 2-tailed Student *t* test (D). ns, not significant.

Downloaded from http://ashpublications.org/blood/article-pdf/139/18/2797/1895455/bloodbld2021013925.pdf by guest on 29 September 2023

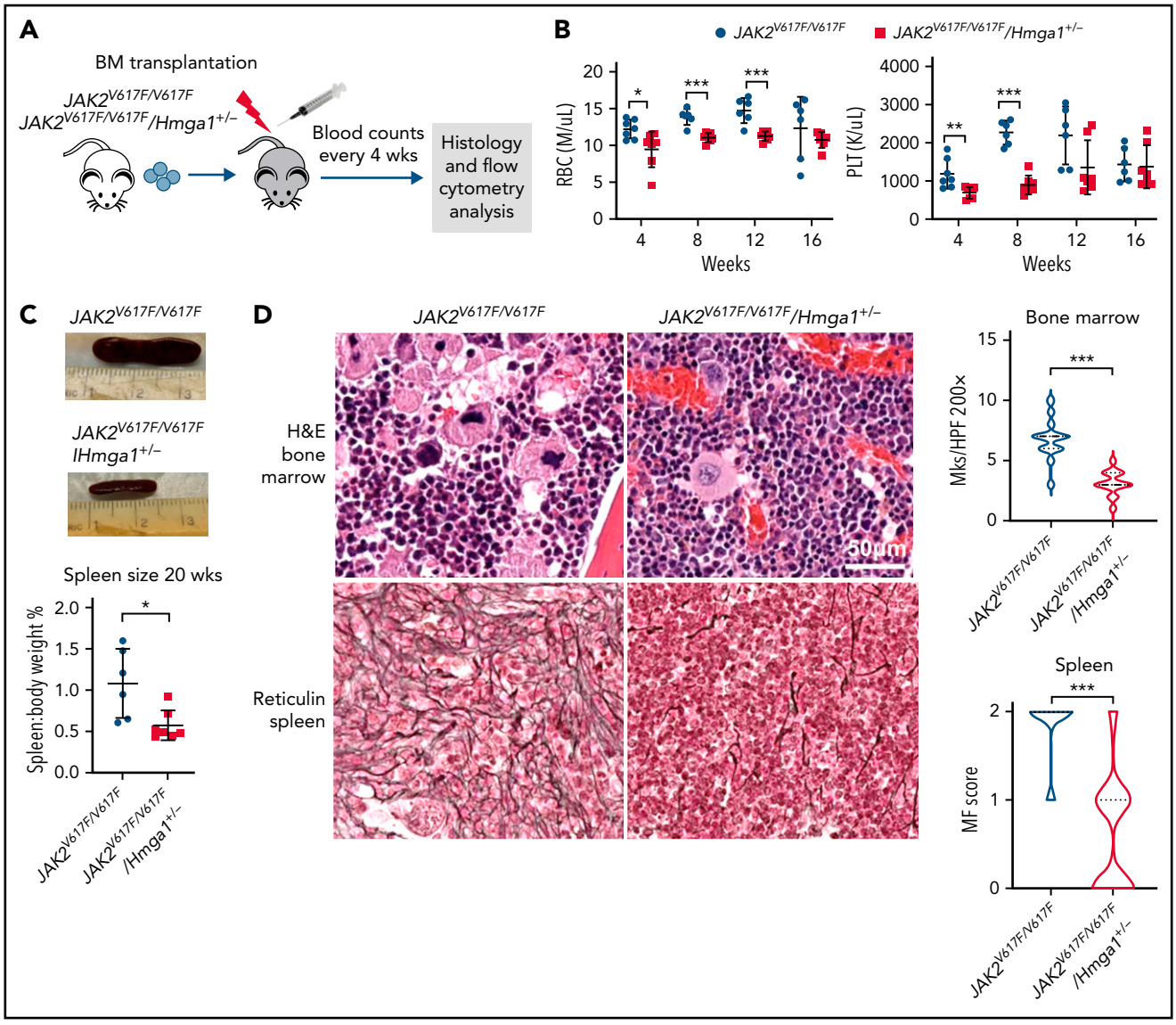

Figure 3. *Hmga1* deficiency prevents MPN phenotypes and expansion of long-term HSC and myeloid progenitors from *JAK2*$^{V617F/V617F}$ mice in a transplantation model. (A) Experimental design to determine *Hmga1* function in transplantation model. (B) Red blood cell (RBC) and platelet (PLT) counts from PB of age-matched recipients transplanted with *JAK2*$^{V617F/V617F}$ or *JAK2*$^{V617F/V617F}$/*Hmga1*$^{+/-}$ BM cells (n = 6 or 7 per group). (C) Representative spleens and relative spleen size (mean ± standard deviation [SD]) in recipient mice transplanted with *JAK2*$^{V617F/V617F}$ or *JAK2*$^{V617F/V617F}$/*Hmga1*$^{+/-}$ BM cells. (D) Representative BM (humerus; hematoxylin and eosin [H&E] stain) and spleen fibrosis (reticulin staining). Scale bar, 50 μm (left and middle panels). Megakaryocyte numbers per high-power field (Mks/HPF) in BM (humerus; mean ± SD) and splenic fibrosis scores (mean ± SD) from recipient mice transplanted with *JAK2*$^{V617F/V617F}$ or *JAK2*$^{V617F/V617F}$/*Hmga1*$^{+/-}$ BM cells (n = 6 or 7 per group). (E) Representative flow cytometry plots of BM HSPC. Flow cytometric analysis (mean ± SD) assessed in BM or spleen from recipient mice transplanted with *JAK2*$^{V617F/V617F}$ or *JAK2*$^{V617F/V617F}$/*Hmga1*$^{+/-}$ BM cells (n = 6 or 7 per group). (F) t-SNE plot of LSK transcriptomes from scRNAseq colored by clusters. The 2 genotypes (*JAK2*$^{V617F/V617F}$ and *JAK2*$^{V617F/V617F}$/*Hmga1*$^{+/-}$) are superimposed (left panel). t-SNE plot from *JAK2*$^{V617F/V617F}$ (middle panel) and *JAK2*$^{V617F/V617F}$/*Hmga1*$^{+/-}$ (right panel) are shown separately to highlight the variation in distribution among the clusters. *Hmga1* heterozygous deficiency decreases clusters with markers of HSC (cluster 7), megakaryocyte-biased progenitors (cluster 8), and megakaryocyte/erythroid-biased progenitors (clusters 5-6), while increasing clusters with lymphoid-biased progenitors (clusters 0 and 1). The clusters with the greatest differences across genotype are outlined. The table shows the fraction of LSK cells in clusters grouped by genotype (*JAK2*$^{V617F/V617F}$ vs *JAK2*$^{V617F/V617F}$/*Hmga1*$^{+/-}$); *P* values show differences between genotypes in clusters grouped by cell identity. **P* < .05, ***P* < .01, ****P* < .001, Mann–Whitney *U* test (B-C,E), 2-tailed Student *t* test (D).

activation of the +9.5 enhancer region upstream of the *GATA2* minimal promoter (*GATA2*-1S). *GATA2*-1S showed low activity, which remained unchanged by *HMGA1* silencing, whereas reporter activity increased more than three-fold when the +9.5 enhancer site A was present and more than four-fold when sites A and B were included; accordingly, +9.5 reporter activity decreased upon *HMGA1* silencing (Figure 4K). Together, these results indicate that HMGA1 binds directly to sites near the *GATA2* +9.5 enhancer, increasing chromatin accessibility and recruiting active histone marks (H3K4me1/H3K4me3) to induce *GATA2*.

GATA2 silencing phenocopies HMGA1 deficiency, and *GATA2* restoration partially rescues antileukemogenic effects of HMGA1 depletion

To determine whether *GATA2* is required for HMGA1 function, we depleted *GATA2* in *JAK2*^{V617F} AML cell lines (DAMI, SET-2,

Downloaded from http://ashpublications.org/blood/article-pdf/139/18/2797/1895455/bloodbld2021013925.pdf by guest on 29 September 2023

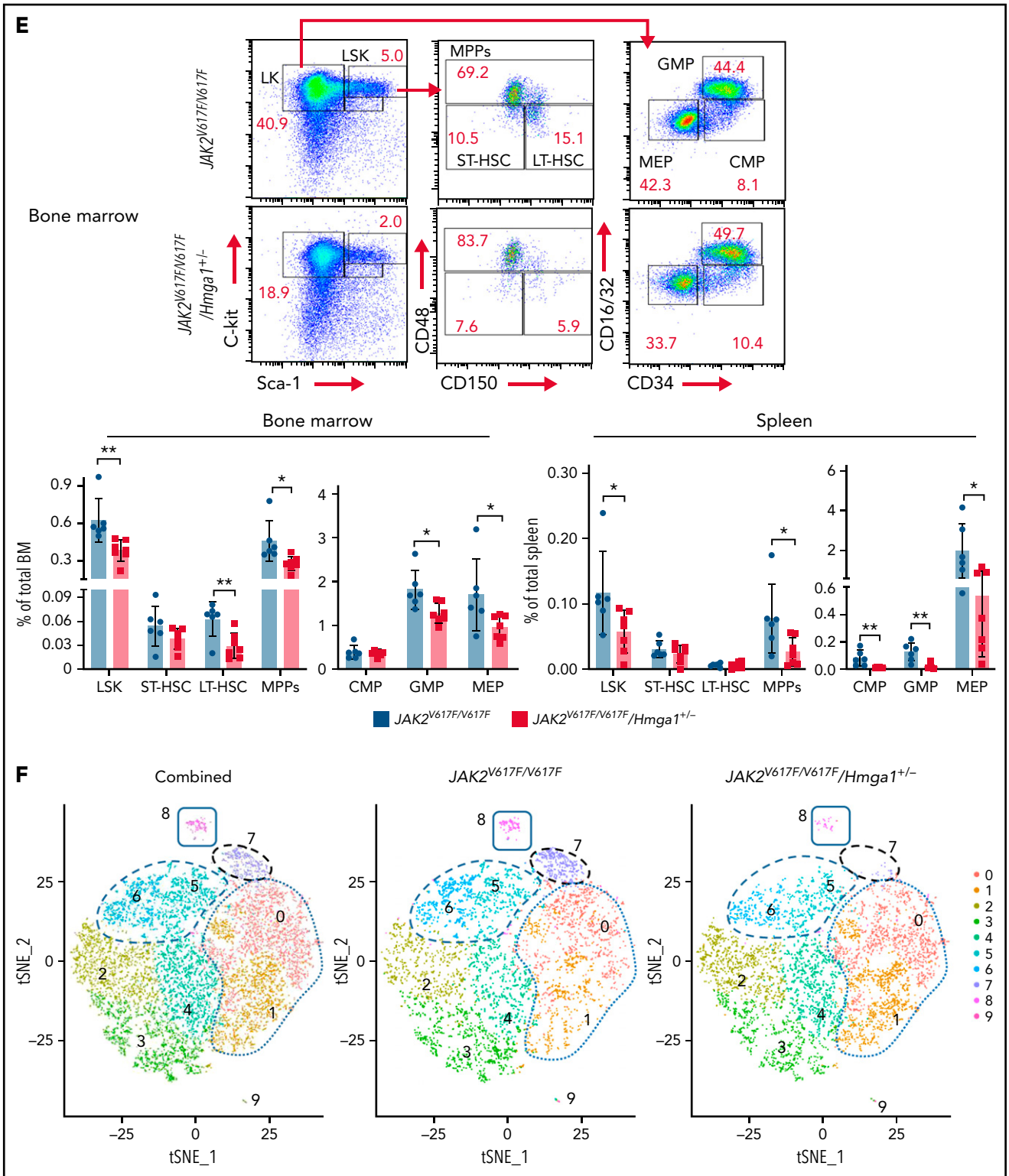

	$JAK2^{V617F/V617F}$	$JAK2^{V617F/V617F}/Hmga1^{+/-}$	*p*-value
HSC	0.082	0.006	<0.00001
Lymphoid-biased progenitor	0.295	0.427	<0.00001
Megakaryocyte/Erythroid biased progenitor	0.192	0.121	<0.00001
Megakaryocyte-biased progenitor	0.027	0.011	<0.00001
Monocyte-biased progenitor	0.003	0.001	0.0053
Myeloid-biased progenitor	0.401	0.435	0.00071

Figure 3. (continued)

Downloaded from http://ashpublications.org/blood/article-pdf/139/18/2797/1895455/bloodbld2021013925.pdf by guest on 29 September 2023

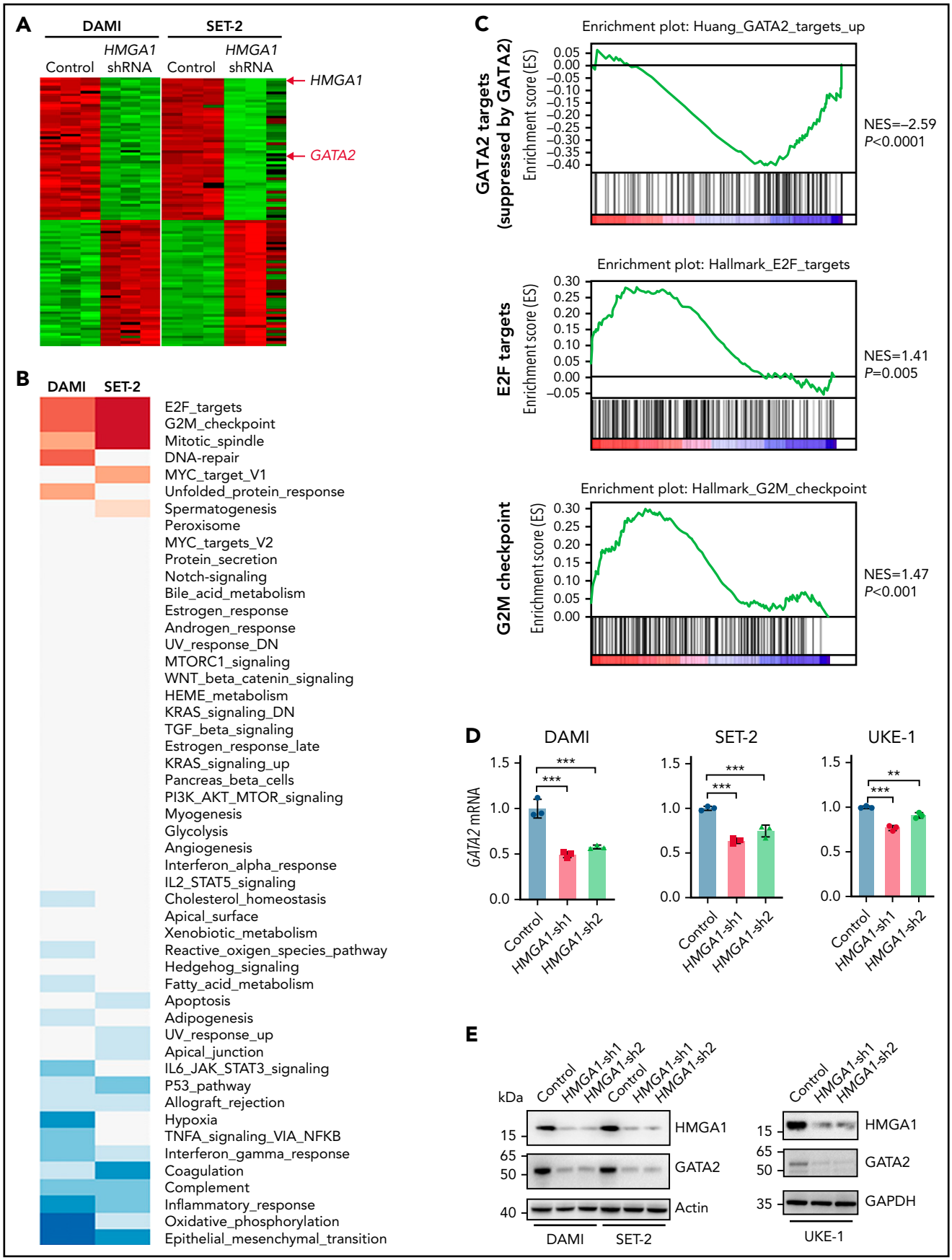

Figure 4.

Downloaded from http://ashpublications.org/blood/article-pdf/139/18/2797/1895455/bloodbld2021013925.pdf by guest on 29 September 2023

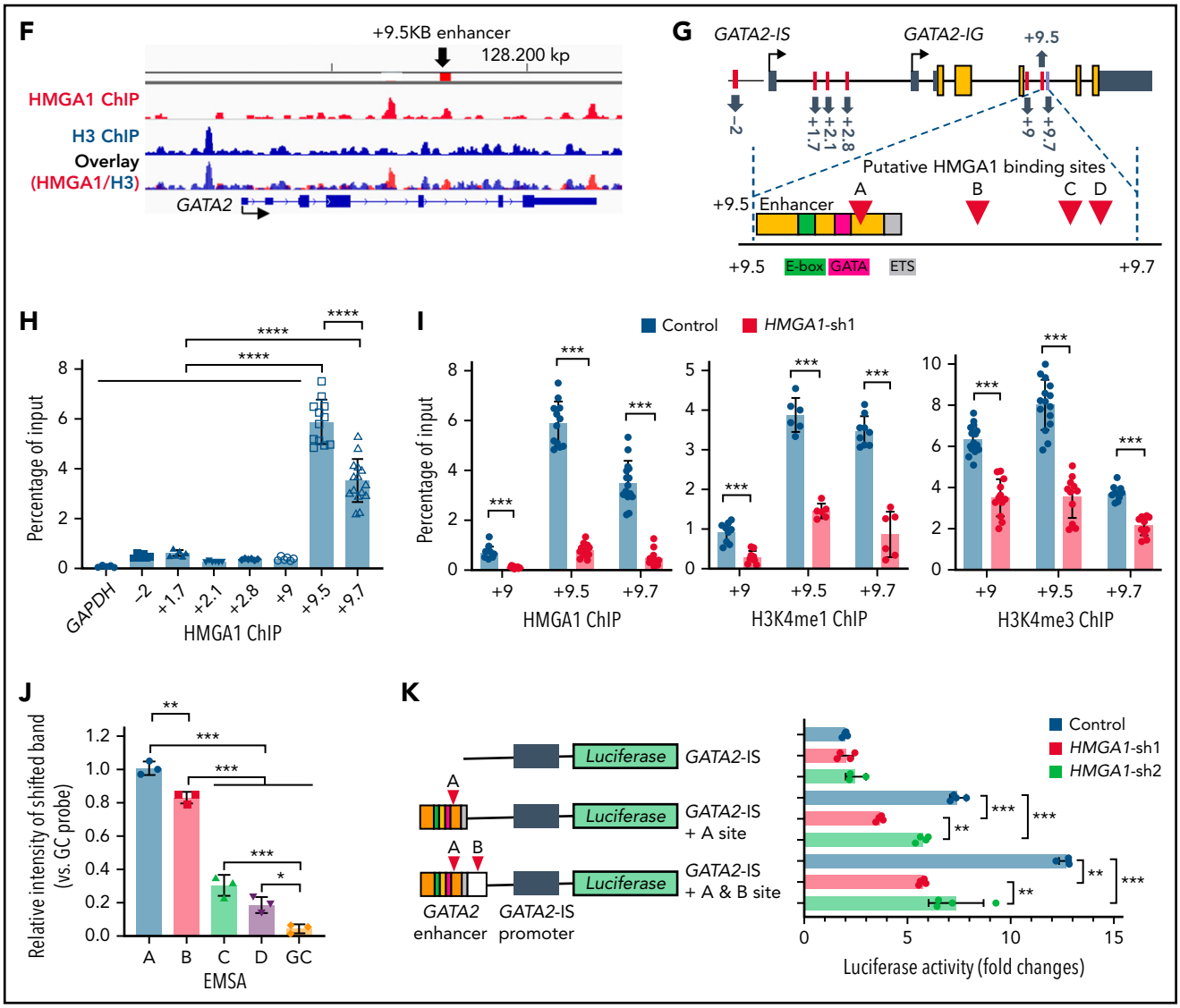

Figure 4. HMGA1 transcriptional networks are involved in cell fate and cell cycle progression. (A) Heat map showssubsets of differentially expressed genes that are upregulated or downregulated by HMGA1 in DAMI and SET-2 *JAK2*^{V617F} AML cell lines. (B) HMGA1 transcriptional networks are enriched for gene sets involved in cell cycle progression (E2F targets, mitotic spindle, G2M checkpoint, MYC targets) and cell fate decisions (GATA2 networks and *GATA2*). The left column was derived from DAMI and the right column from SET-2 . (C) GSEA performed from transcriptomes from DAMI and SET-2 , with or without *HMGA1* silencing (control vs *HMGA1*-sh1). Adjusted *P* values and normalized enrichment scores (NES) are shown. (D) Relative *GATA2* expression (mean ± standard deviation [SD]) assessed from 2 independent experiments performed in triplicate (quantitative polymerase chain reaction) in DAMI, SET-2, and UKE-1 cells, with or without *HMGA1* silencing (control vs *HMGA1*-sh1 or *HMGA1*-sh2). *GAPDH* was used to control for loading. (E) Western blots for HMGA1, GATA2, and β-actin (loading control) protein levels from DAMI, SET-2, and UKE-1 cells, with or without *HMGA1* silencing (control vs *HMGA1*-sh1 or *HMGA1*-sh2). Western blots were performed 3 times with similar results; a representative blot is shown. Size markers (kDa) are indicated. (F) Integrative Genomics Viewer browser view of HMGA1 ChIPseq (top, red), H3 ChIPseq (middle, blue), and overlay (bottom) across the *GATA2* locus from DAMI WT cells. (G) Schematic representation of the human *GATA2* region with 6 regions (red) that include in silico–predicted HMGA1 DNA binding motifs (upper part of panel). *GATA2*-1S and *GATA2*-1G promoters are shown with black arrows to indicate the transcriptional start sites (TSS). The black box represents the untranslated region, and the orange boxes are coding exons. Numbers indicate the nucleotide positions relative to the *GATA2-IS* TSS. Schematic representation of region with 4 putative HMGA1 binding motifs within a 230-bp fragment of the *GATA2* +9.5 enhancer area (lower part of panel). The 4 predicted HMGA1 binding motifs (A-D) are marked with red arrowheads. The +9.5 enhancer (yellow) with 3 DNA binding motifs (E-box, green; GATA, pink; and erythroblast transformation specific [ETS], gray) are also shown. (H) HMGA1 enrichment at the +9.5 enhancer and +9.7 regions within the *GATA2* locus by ChIP-PCR in DAMI cells, with or without *HMGA1* silencing, performed in triplicate from 3 independent experiments. Results (mean ± SD) are the percentage recovered from the total input DNA (% input). *GAPDH* promoter (left lane) was used as a negative control for HMGA1 occupancy. (I, left) HMGA1 ChIP-PCR assays comparing occupancy at +9, +9.5, and +9.7 regions using DAMI cells, with or without *HMGA1* silencing (control vs *HMGA1*-sh1). Results (mean ± SD) are presented as the percentage recovered from the total input DNA (% input) performed in triplicate in 3 independent experiments. (I, center and right) HMGA1 recruits active histone marks at +9, +9.5, and +9.7 regions with enrichment for H3K4me1 (Middle) and H3K4me3 (Right), by ChIP-PCR in control DAMI cells with abundant HMGA1; active marks are depleted with *HMGA1* silencing (control vs *HMGA1*-sh1). ChIP-PCR was performed in triplicate in 3 independent experiments. (J) HMGA1 DNA binding activity to probe sequences from 4 putative binding sites near the +9.5 enhancer by electrophoretic mobility shift assay. HMGA1-DNA complexes from 3 independent experiments (mean ± SD) were compared quantitatively in the bar graph. A GC-rich probe was used as a negative control. (K) HMGA1 induces *GATA2* enhancer sequences linked to a luciferase reporter gene in control DAMI cells, with decreased reporter gene activation with *HMGA1* silencing (control vs *HMGA1*-sh1 or *HMGA1*-sh2). Constructs include *GATA2*-1S promoter, *GATA2*-1S promoter plus HMGA1 binding motif A, and *GATA2*-1S promoter plus HMGA1 binding motifs A and B. Results (mean ± SD) represent 2 experiments performed with 4 replicates. **P* < .05, ***P* < .01,****P* < .001, *****P* < .0001, 2-tailed Student *t* test (D,I), 1-way ANOVA, followed by Tukey's multiple-comparison test (H,J-K).

Downloaded from http://ashpublications.org/blood/article-pdf/139/18/2797/1895455/bloodbld2021013925.pdf by guest on 29 September 2023

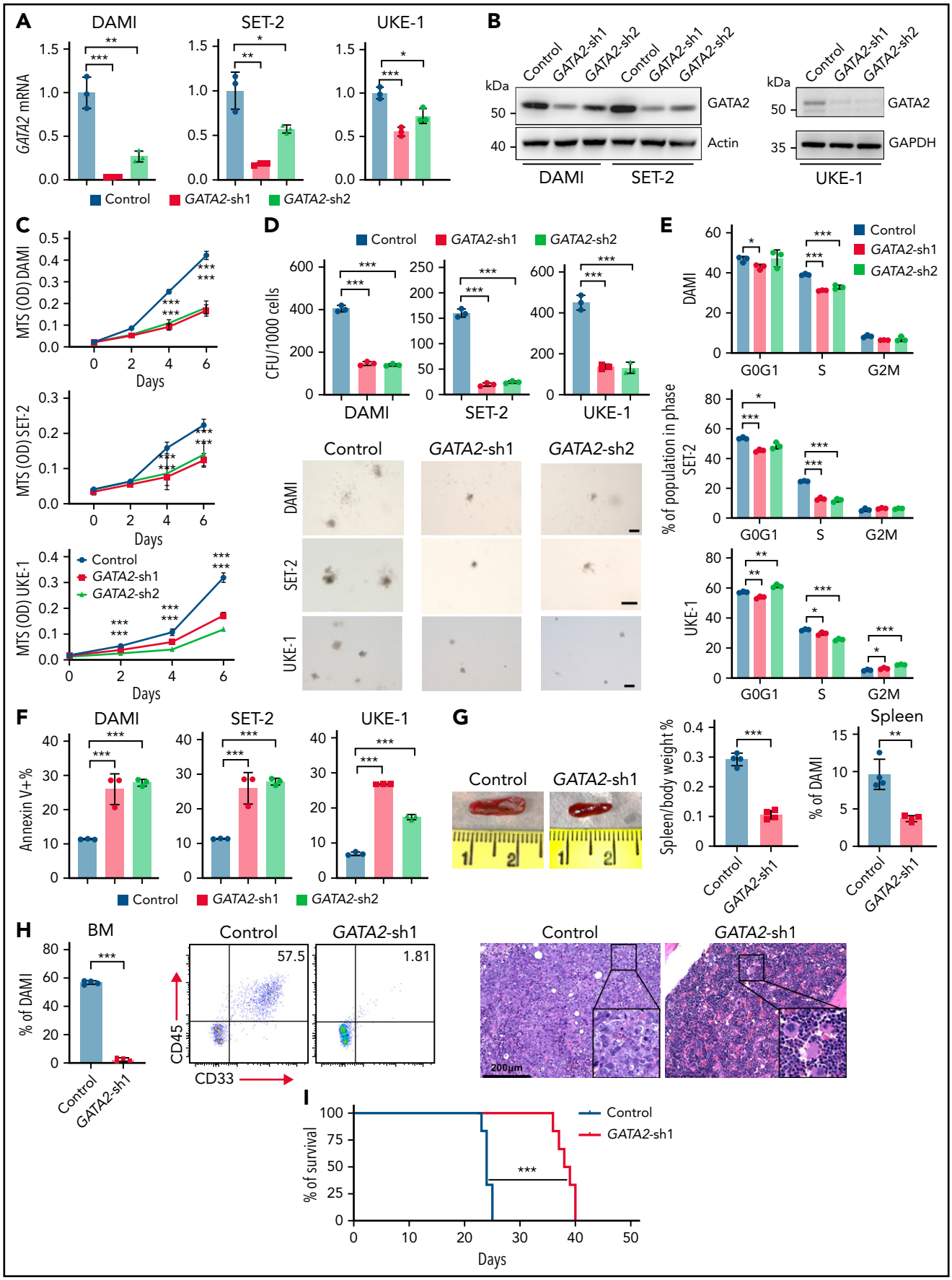

Figure 5.

Downloaded from http://ashpublications.org/blood/article-pdf/139/18/2797/1895455/bloodbld2021013925.pdf by guest on 29 September 2023

and UKE-1) via shRNA targeting of 2 different sequences. Silencing *GATA2* decreases proliferation, clonogenicity, and the frequency of cells in S phase while increasing apoptosis, recapitulating phenotypes observed with *HMGA1* depletion (Figure 5A-F; supplemental Figure 8). *GATA2* deficiency also disrupts the leukemogenic potential of DAMI cells, decreasing splenomegaly and leukemic engraftment (BM, spleen); moreover, survival was prolonged in recipients of DAMI cells with *GATA2* silencing (Figure 5G-I). Similar to our results with *HMGA1*, engrafted leukemic cells from the pool of cells with *GATA2* silencing express higher *GATA2* compared with the injected cells, suggesting that a critical level of *GATA2* is required for engraftment (supplemental Figure 9). Collectively, our results indicate that *GATA2* is an important mediator of HMGA1 in these *JAK2*^{V617F} AML models.

To determine whether restoring GATA2 rescues anti-leukemogenic phenotypes mediated by *HMGA1* silencing, we engineered DAMI, SET-2, and UKE-1 cells with *HMGA1* silencing and concurrent expression of *GATA2*, such that *GATA2* levels (messenger RNA, protein) approximate those of parental cells. *GATA2* partially rescues phenotypes associated with *HMGA1* depletion, increasing, but not restoring, clonogenicity in *JAK2*^{V617F} AML cell lines (Figure 6A-C; supplemental Figure 10A). *GATA2* rescues the frequency of apoptotic cells to baseline levels, although proliferation and cell cycle progression were unchanged (Figure 6D; supplemental 10B-C). *GATA2* restoration also partially rescues the antileukemogenic effects of *HMGA1* silencing (Figure 6E-F). As before, disease latency was shortest in recipients of DAMI cells with endogenous expression of *HMGA1* and *GATA2* (median survival, 24 days) and was longest in recipients of cells with *HMGA1* depletion (median survival, 38 days). The recipients of leukemic cells with *HMGA1* silencing and *GATA2* overexpression had intermediate survival (32.5 days; $P < .01$). *GATA2* restoration increases the frequency of BM-engrafted DAMI cells more than two-fold compared with those with *HMGA1* depletion, although splenic engraftment was unchanged (Figure 6F; supplemental Figure 10D). These results demonstrate that *GATA2* partially mediates HMGA1 function in models of *JAK2*^{V617F} AML.

HMGA1 networks are activated with leukemic transformation in human MPN

To determine the significance of the *HMGA1-GATA2* network in human MPN progression, we compared the expression of *HMGA1* and *GATA2* in primary human MPN. Strikingly, *GATA2* and *HMGA1* are coexpressed and positively correlated via RNA-seq from PBMCs from a cohort of matched patients with MF that transformed to AML (n = 11) (Figure 6Gi-ii).[26] Further, this relationship was validated in independent studies (Figure 6Giii-iv; supplemental Figure 11): (1) *HMGA1* and *GATA2* are coexpressed and upregulated in BM CD34$^+$ cells with progression from PV or ET to MF (GSE103237),[79] (2) *HMGA1* and *GATA2* are upregulated in PB CD34$^+$ cells from MF compared with age-matched healthy controls by scRNAseq (GSE144568),[71] and, (3) in another scRNAseq cohort with greater sequencing depth, *HMGA1* and *GATA2* are coexpressed and upregulated in *JAK2*-mutated PB CD34$^+$ cells from MF compared with unmutated CD34$^+$ cells from the same patients or CD34$^+$ cells from unaffected individuals (GSE122198).[70]

Next, we identified the pathways that are activated in human MPN. In the matched cohort of MF to AML, most leukemic samples show activation of pathways distinct from those in MF, and there was a striking overlap with pathways activated in leukemia and HMGA1 networks identified in our cell-based models. Specifically, networks driving cell cycle progression pathways are activated after transformation to AML, including the most significant HMGA1 pathways (G2M, mitotic spindle, E2F; Figure 6H). Pathways repressed in the leukemic samples overlap with those repressed by HMGA in *JAK2*^{V617F} AML cell-based models, including interferon-γ (data not shown). Furthermore, *HMGA1* transcript levels correlate with HMGA1 pathway activation in the primary MPN AML cells (Figure 6H). Similarly, the scRNAseq cohorts show activation of HMGA1 networks (E2F targets, G2M checkpoint, DNA repair), including *GATA2* with progression to MF.[70,71] Together, these results implicate HMGA1 as a driver of transcriptional networks required in human MPN progression.

HMGA1 depletion enhances responses to the JAK/STAT inhibitor ruxolitinib

Next, we determined whether HMGA1 deficiency enhances sensitivity to the JAK/STAT inhibitor ruxolitinib in *JAK2*^{V617F} AML. First, we found that the concentration at which 50% of DAMI cells stop proliferating with ruxolitinib treatment decreases upon *HMGA1* depletion (406.5 nM vs 204.8 nM; $P < .001$) (Figure 7A). Second, we tested the effects of ruxolitinib with *HMGA1* silencing on leukemogenesis in vivo. Therapy was delivered via chow supplemented with ruxolitinib (2000 mg INCB01842 per kilogram diet) to provide doses shown to reach therapeutic

Figure 5. *GATA2* silencing phenocopies *HMGA1* silencing in preclinical models of *JAK2*^{V617F} MPN AML. (A) Relative *GATA2* expression (mean ± standard deviation [SD]) from 2 experiments performed in triplicate (quantitative polymerase chain reaction) in DAMI, SET-2, and UKE-1 cells, with or without *HMGA1* silencing (control vs *GATA2*-sh1 or *GATA2*-sh2). *GAPDH* was used as a loading control. (B) Western blots of GATA2, β-actin, and GAPDH (loading control) protein levels from DAMI, SET-2, and UKE-1 cells, with or without *GATA2* silencing (control vs *GATA2*-sh1 or *GATA2*-sh2). Western blots were performed 3 times with similar results; a representative blot is shown. Size markers (kDa) are indicated. (C) Proliferation (mean ± SD) by MTS [3-(4,5-dimethylthiazol-2-yl)-5-(3-carboxymethoxyphenyl)-2-(4-sulfophenyl)-2H-tetrazolium; Promega)] assay in DAMI, SET-2 and UKE-1 cells, with or without *GATA2* silencing (control vs *GATA2*-sh1 or *GATA2*-sh2), at the indicated time points. (D) Colony-forming units (CFU; mean ± SD) in DAMI, SET-2, and UKE-1 cells, with or without *GATA2* silencing (control vs *GATA2*-sh1 or *GATA2*-sh2), in 2 experiments performed in triplicate. Representative images of colony formation after silencing *GATA2* by delivery of a lentiviral vector expressing shRNA targeting *GATA2* (control vs *GATA2*-sh1 or *GATA2*-sh2) are shown. Scale bars, 200 μm. (E) Edu (5-ethynyl-2′-deoxyuridine) cell cycle (mean ± SD) by flow cytometry assessed in DAMI, SET-2, and UKE-1 cells, with or without *GATA2* silencing (control vs *GATA2*-sh1 or *GATA2*-sh2), in 2 experiments performed in triplicate. (F) Annexin V apoptosis by flow cytometry assessed in DAMI, SET-2, and UKE-1 cells, with or without *GATA2* silencing (control vs *GATA2*-sh1 or *GATA2*-sh2) in 2 experiments. (G) Representative images of spleens and relative spleen size (mean ± SD); leukemia cell engraftment (mean ± SD) assessed by flow cytometry in spleen from NSG mice injected with DAMI cells with or without *GATA2* silencing (control vs *GATA2*-sh1; n = 4 per group). (H) Leukemia cell engraftment assessed by flow cytometry (mean ± SD) in BM from NSG mice injected with DAMI cells, with or without *GATA2* silencing (control vs *GATA2*-sh1; n = 4 per group). Representative flow cytometry plots from each group and hematoxylin and eosin–stained BM are shown. Scale bar, 200 μm. (I) Survival analysis by Kaplan-Meier estimate assessed in NSG mice injected with DAMI cells transduced with lentivirus (control: median survival, 24 days vs *GATA2*-sh1: median survival, 38.5 days; n = 6 per group). *$P < .05$, **$P < .01$, ***$P < .001$, ***$P < .001$, 2-tailed Student *t* test (A,C-H), log-rank (Mantel-Cox) test (I).

Downloaded from http://ashpublications.org/blood/article-pdf/139/18/2797/1895455/bloodbld2021013925.pdf by guest on 29 September 2023

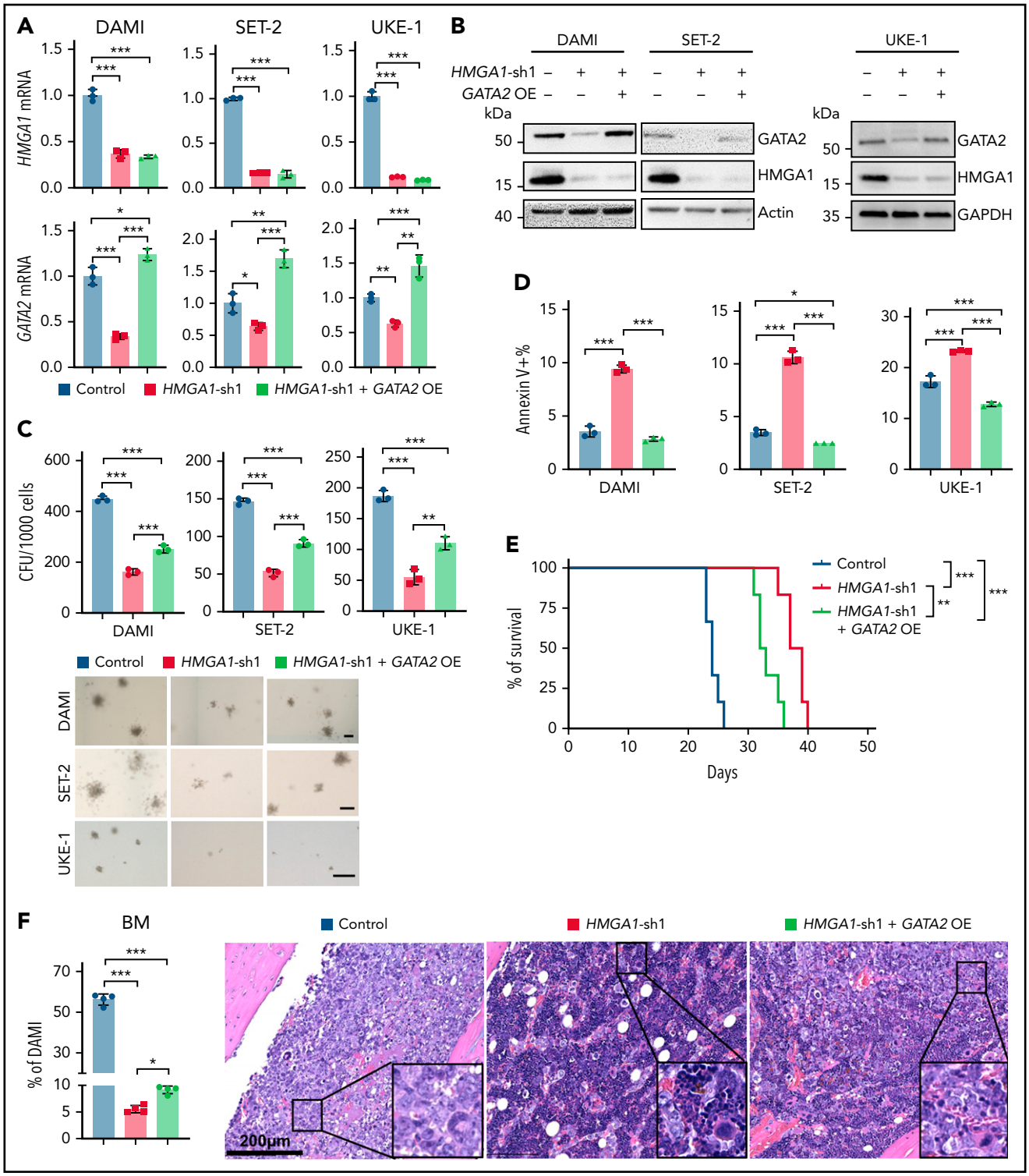

Figure 6. *GATA2* restoration partially rescues antileukemogenic effects of *HMGA1* silencing; *GATA2* and *HMGA1* are coexpressed in primary MPN and HMGA1 networks and are activated in leukemic blasts from patients with MPN. (A) Relative *HMGA1* and *GATA2* expression (mean ± standard deviation [SD]) from 2 experiments performed in triplicate (quantitative polymerase chain reaction) in DAMI, SET-2, and UKE-1 cells (control vs *HMGA1*-sh1 vs *HMGA1*-sh1 + *GATA2* overexpression [OE]). *GAPDH* was used to control for loading. (B) Western blots of HMGA1, GATA2, β-actin, and GAPDH (loading control) protein levels from DAMI, SET-2, and UKE-1 cells transduced with lentivirus (control vs *HMGA1*-sh1 vs *HMGA1*-sh1 + *GATA2* OE). Western blots were performed 3 times with similar results; a representative blot is shown. Size markers (kDa) are indicated. (C) Colony-forming units (CFU; mean ± SD) from DAMI, SET-2, and UKE-1 cells (control vs *HMGA1*-sh1 vs *HMGA1*-sh1 + *GATA2* OE) in 2 experiments. Representative images of colonies are shown. Scale bars, 200 μm. (D) Annexin V apoptosis by flow cytometry in DAMI, SET-2, and UKE-1 cells (control vs *HMGA1*-sh1 vs *HMGA1*-sh1 + *GATA2* OE) in 2 experiments. (E) Survival curve (Kaplan-Meier plots) in NSG mice injected with DAMI cells (control vs *HMGA1*-sh1 vs *HMGA1*-sh1 + *GATA2* OE; n = 6). (F) Leukemia cell engraftment assessed by flow cytometry (mean ± SD) in BM from NSG mice injected with DAMI cells transduced with lentivirus (control vs *HMGA1*-sh1 vs *HMGA1*-sh1 + *GATA2* OE; n = 4 per group). Representative BM histology (hematoxylin and eosin stain) from each group are shown. Scale bar, 200 μm. (Gi) *HMGA1* and *GATA2* expression (RNAseq) from PBMCs from a cohort of matched patient samples

Downloaded from http://ashpublications.org/blood/article-pdf/139/18/2797/1895455/bloodbld2021013925.pdf by guest on 29 September 2023

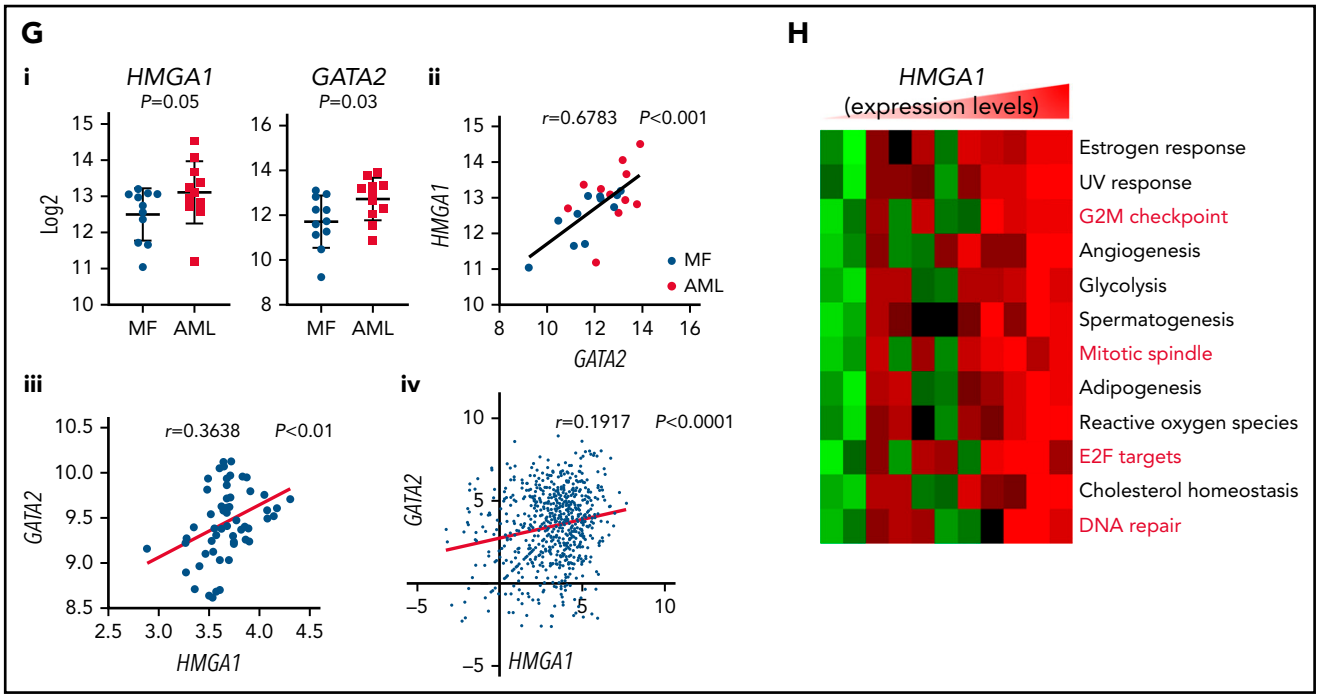

Figure 6 (continued) with MF that progressed to AML (n = 11 per group). (Gii) *HMGA1* and *GATA2* are positively correlated ($P < .001$); Pearson correlation coefficient. (Giii) *HMGA1* and *GATA2* are positively correlated ($P < .01$) in *JAK2*-mutant CD34$^+$ BM cells from patients with ET or PV and unaffected individuals (GSE103237); Pearson correlation coefficient. (Giv) *HMGA1* and *GATA2* in *JAK2*-mutant CD34$^+$ PB cells from patients with MF compared with unmutated CD34$^+$ cells from the same patients (n = 8) or unaffected individuals (n = 2) by scRNAseq (GSE122198). Each dot represents the expression value for each single cell ($P < .0010$); Pearson correlation coefficient. (H) Transcriptional networks activated in MPN PBMCs after leukemic transformation correlate positively with *HMGA1* expression levels ($P < .05$; Spearman correlation > 0.6) and overlap with the top HMGA1 networks (red) identified in *JAK*^{V617F} MPN cell lines (DAMI, SET-2). *$P < .05$, **$P < .01$, ***$P <$. 001; 1-way ANOVA, followed by Tukey's multiple-comparison test (A-D,F), log-rank (Mantel-Cox) test, followed by Bonferroni correction (E).

levels in mice[89,90]; control chow was identical except it lacked ruxolitinib. We included 4 groups: (1) DAMI control, control chow, (2) DAMI control, ruxolitinib chow, (3) DAMI with *HMGA1* depletion, control chow, and (4) DAMI with *HMGA1* depletion, ruxolitinib chow. After 24 days of therapy, we assessed leukemic engraftment. Mice injected with control DAMI cells and placed on control chow had the highest leukemic burdens in spleen and BM, whereas recipients of DAMI cells with *HMGA1* silencing and ruxolitinib treatment showed the lowest engraftment and spleen sizes, followed by recipients of DAMI cells with *HMGA1* silencing and control chow (Figure 7B-C; supplemental Figure 12). Moreover, survival is prolonged in recipients of AML cells with *HMGA1* silencing and ruxolitinib therapy (Figure 7D).

We also tested ruxolitinib in the *JAK*$^{V617F/V617F}$ chronic MPN model with therapy beginning at 16 to 20 weeks of age when erythrocytosis and splenomegaly are well established (supplemental Figure 13A). Ruxolitinib decreased splenomegaly and fibrosis in *JAK*$^{V617F/V617F}$ mice (Figure 7E-F). In the *JAK*$^{V617F/V617F}$ model, *Hmga1* heterozygosity decreases splenomegaly and prevents fibrosis (supplemental Figure 13B). Spleen sizes decrease further with ruxolitinib in *JAK*$^{V617F/V617F}$ mice with *Hmga1* heterozygosity (supplemental Figure 13). There were decreases in leukocytosis with modest changes in erythrocytosis in both models (supplemental Figure 13A). Together, these results indicate that *HMGA1* silencing or *Hmga1* haploinsufficiency enhances sensitivity to ruxolitinib in preclinical MPN models and strongly support HMGA1 as a rational therapeutic target.

Discussion

We discovered a novel role for HMGA1 as an epigenetic switch involved in *JAK2*^{V617F} MPN progression. Using shRNA-mediated or CRISPR/Cas9-mediated gene silencing in *JAK2*^{V617F} models, we found that HMGA1 deficiency: 1) decreases proliferation, clonogenicity, and leukemic engraftment; 2) represses transcriptional networks involved in cell cycle progression, proliferation, and GATA2 function; and, 3) most importantly, enhances sensitivity to the JAK inhibitor ruxolitinib in disrupting leukemic engraftment and prolonging survival. We validated the significance of HMGA1 in human MPN because *HMGA1* and downstream pathways, including *GATA2*, are upregulated during progression in independent cohorts. Moreover, HMGA1 transcriptional pathways are activated in *JAK2*^{V617F} CD34$^+$ cells compared with those lacking mutant *JAK*, and in matched MF samples after transformation to leukemia, further illuminating HMGA1 as a promising therapeutic target. The enhanced response to ruxolitinib by HMGA1 depletion is particularly striking in AML because ruxolitinib is not effective in patients with MPN after leukemic transformation.

Surprisingly, *Hmga1* haploinsufficiency prevents MF in chronic MPN models, reducing erythrocytosis, megakaryocyte hyperplasia, splenomegaly, and fibrosis, while dampening expansion of *JAK2*^{V617F} mutant stem and progenitor cells. This was unexpected for 2 reasons; first, although *HMGA1* is a potent oncogene and driver of progression in aggressive solid tumor modes, its role in clonal hematopoiesis and more indolent

Downloaded from http://ashpublications.org/blood/article-pdf/139/18/2797/1895455/bloodbld2021013925.pdf by guest on 29 September 2023

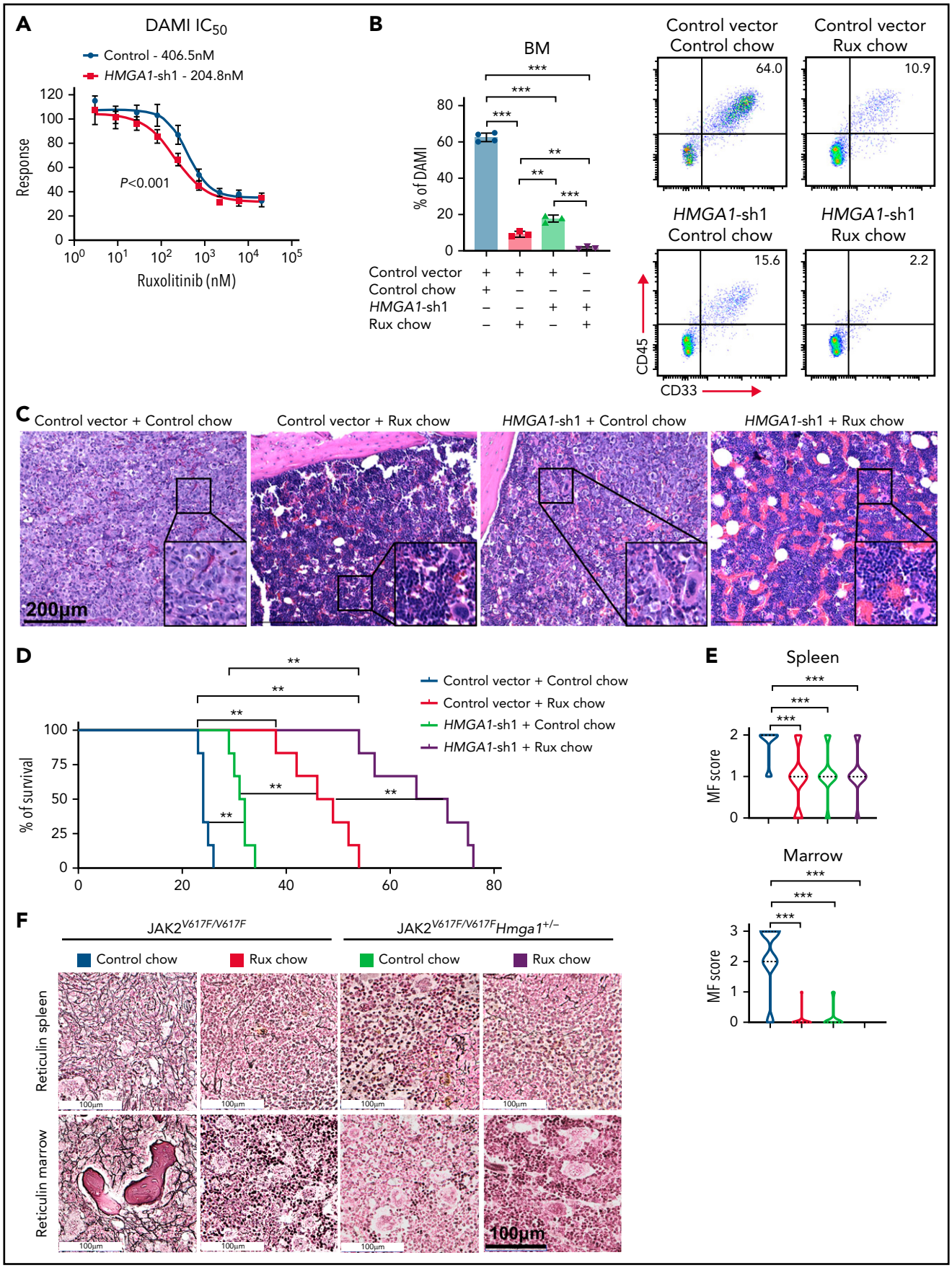

Figure 7.

Downloaded from http://ashpublications.org/blood/article-pdf/139/18/2797/1895455/bloodbld2021013925.pdf by guest on 29 September 2023

neoplasia had not been demonstrated. Second, most studies focusing on *HMGA1* in tumor cells rely on gene silencing to low levels. Thus, we did not anticipate that reducing levels by only 50% would so profoundly impact progression. Moreover, the normal steady-state hematopoiesis in *Hmga1* heterozygous mice suggests that pharmacologic modulation of HMGA1 to this degree is a plausible therapeutic end point, although specific inhibitors of HMGA1 are not yet available.

To uncover actionable mechanisms mediated by HMGA1, we investigated downstream transcriptomic and epigenetic changes, which identified HMGA1-dependent transcriptional networks governing cell cycle progression and cell fate, including E2F and GATA2 targets. Intriguingly, a recent study using mutant MPL^{W515L} murine models identified E2F networks in MPN progression that were targeted by inhibiting PRMT5, a protein arginine methyltransferase,[25] although it remains to be shown whether similar approaches disrupt HMGA1 networks. Instead, we focused on the GATA2 master regulator, given its association with HSC function and poor outcomes in AML.[84-87]

HMGA1 aberrantly induces *GATA2* in human JAK^{V617F} AML cell lines and murine models. Moreover, this pathway is activated in human MPN progression. HMGA1-mediated induction of *GATA2* could preclude normal GATA1 function in HSPCs and megakaryocytes, thereby mimicking the GATA1-low phenotype that causes MF in mice.[91-93] Low GATA1 protein levels were observed in megakaryocytes from patients with MF.[92,93] We did not test the effects of *Gata2* loss in our JAK^{V617F} mice because *Gata2* deficiency disrupts hematopoiesis. Modulating HMGA1 provides a more attractive therapeutic approach. Notably, repressing *GATA2* recapitulates many phenotypes observed with *HMGA1* silencing, and restoring *GATA2* only partially rescues anti-leukemic effects of HMGA1 depletion, demonstrating that GATA2 is only one HMGA1 effector in MPN. Indeed, RNA-seq, ChIPseq and ATACseq revealed other networks that are involved in proliferation; thus, pharmacologically targeting these pathways may be beneficial.

The role of HMGA1 in orchestrating the assembly of specific histone marks had not been studied in detail. We found that HMGA1 enhances chromatin accessibility and recruits histone marks associated with gene activation, including H3K3me3 (for active promoters) and H3K4me1 (active enhancers). Previous studies focused on HMGA1 occupancy upstream of minimal promoters,[28,29] although we discovered HMGA1 occupancy at the *GATA2* +9.5 distal enhancer, suggesting that HMGA1 activates or "rewires" enhancer function when overexpressed during MPN progression.

In $JAK2^{V617F}$ mice, *Hmga1* haploinsufficiency mitigates expansion of HSCs, specific myeloid progenitors (MEPs, GMPs), and megakaryocytes, without affecting CLPs. scRNAseq corroborated these results, indicating that *Hmga1* haploinsufficiency decreased clusters with HS and megakaryocyte/erythroid-biased markers while expanding those with lymphoid-biased markers. HSCs and MEPs represent key progenitors in diverse MPN models of MF, including mice expressing $JAK2^{V617F}$ or mutant thrombopoietin receptor MPL^{W515L}.[23,94] HMGA1 is also a master regulator in other adult stem cell populations, including intestinal stem cells,[28,33] which rely on many transcription factors that are active in HSCs. Further, intestinal epithelium and hematopoiesis require highly regenerative stem cell pools to replace mature progeny, and *HMGA1* is re-expressed in hematologic and intestinal malignancies where it amplifies stem-like networks.[28,33,54] These data suggest that tightly regulated HMGA1 is critical for stem cell function under homeostatic conditions, whereas mutated genomes, together with *HMGA1* overexpression, foster aberrant proliferation, differentiation, and transformation.

Intriguingly, *HMGA1* was upregulated in early-stage MPN with *JAK2* mutations, but not in *CALR*-mutated early-stage disease. In our Johns Hopkins University cohort, $CD34^+$ AML blasts with the highest *HMGA1* expression also harbor mutant *EZH2* and *ASXL1*, suggesting that other clonal hematopoiesis lesions may induce *HMGA1*. Given the prevalence of clonal hematopoiesis with aging, further studies to investigate *HMGA1* in this setting are warranted. Although *HMGA2* has been studied in myeloid malignancy and clonal hematopoiesis,[95-98] RNAseq revealed barely detectable *HMGA2* transcripts in human DAMI and SET-2 cell lines and very low levels in most primary human MPN samples. Moreover, *Hmga2* deficiency did not impact progression in the $JAK2^{V617F}$ model when crossed to mice with homozygous or heterozygous deficiency of *Hmga2*. Together, our studies implicate *HMGA1*, rather than *HMGA2*, as a primary driver of $JAK2^{V617F}$ MPN progression.

In summary, we report a novel role for *HMGA1* in $JAK2^{V617F}$ AML and MPN progression using diverse models and orthogonal approaches. Mechanistically, HMGA1 induces transcriptional networks that are involved in cell cycle progression and aberrant differentiation, the latter of which includes direct transactivation of *GATA2*. Together, our findings reveal HMGA1 as a new therapeutic target in MPN and open the door to novel therapeutic approaches to prevent disease progression. Because *HMGA1* and *GATA2* are also overexpressed in de novo AML, this pathway may be relevant, more broadly, in myeloid malignancies.

Downloaded from http://ashpublications.org/blood/article-pdf/139/18/2797/1895455/bloodbld2021013925.pdf by guest on 29 September 2023

Figure 7. *HMGA1* silencing enhances responses to the JAK/STAT inhibitor ruxolitinib (Rux), delaying leukemia engraftment and prolonging survival. (A) Dose response curve with 50% inhibitory concentration in DAMI cells, with or without *HMGA1* silencing. (B) Leukemia cell engraftment by flow cytometry (mean ± standard deviation [SD]) in BM from NSG mice injected with DAMI cells, including DAMI controls with control chow, DAMI controls with Rux chow, DAMI cells with *HMGA1* silencing and control chow, and DAMI cells with *HMGA1* silencing and Rux chow (n = 3 or 4 per group). Representative flow cytometry plots from each group are shown. (C) BM (hematoxylin and eosin stain) from each group described above. Scale bar, 200 μm. (D) Survival curves (Kaplan-Meier plots) of NSG mice injected with DAMI cells and treated as follows: DAMI controls with control chow (median survival, 24 days), DAMI controls with Rux chow (median survival, 47.5 days), DAMI cells with *HMGA1* silencing and control chow (median survival, 31.5 days), and DAMI cells with *HMGA1* silencing and Rux chow (median survival 68 days; n = 6 per group). (E) MF scores based on reticulin staining (mean ± SD) in spleen (scale 0-2) and BM (scale 0-3) from $JAK2^{V617F/V617F}$ mice with control chow or rux chow and $JAK2^{V617F/V617F}/Hmga1^{+/-}$ mice with control chow or rux chow mice were assessed. (F) Representative images of spleen (upper panels) and BM (lower panels) from femurs of $JAK2^{V617F/V617F}$ mice with control or rux chow and $JAK2^{V617F/V617F}/Hmga1^{+/-}$ mice with control or rux chow (reticulin stain). Scale bar, 100 μm. *$P < .01$, **$P < .01$, ***$P < .001$, 1-way ANOVA, followed by Tukey's multiple-comparison test (B,E), log-rank (Mantel-Cox) test, followed by Bonferroni correction (D), 2-way ANOVA (F).

Acknowledgments

The authors thank the Mutation Generation and Detection Core at the University of Utah (National Institute of Diabetes and Digestive and Kidney Diseases Cooperative Hematology Specialized Core Center Grant U54DK110858), the Yale Cooperative Centers of Excellence in Hematology (National Institute of Diabetes and Digestive and Kidney Diseases Grant U54DK106857), and the Johns Hopkins University Ross Flow Core (National Institutes of Health Shared Instrument Grants S10OD026859 for Cytek Aurora Full Spectrum Flow Cytometric Analyzer).

This work was supported by National Institutes of Health National Heart, Lung, and Blood Institute grants R01HL145780 (L.M.S.R., A.R.M.) and R01HL143818 (L.M.S.R.), National Institutes of Health National Cancer Institute grant CA232741 (L.M.S.R.), National Institutes of Health National Institute of Diabetes and Digestive and Kidney Diseases grant DK102943 (L.M.S.R.), the MPN Research Foundation (L.R., A.R.M.), the Children's Cancer Research Fund (L.M.S.R.), Alex's Lemonade Stand Foundation (L.M.S.R.), the Allegheny Health Network (L.M.S.R.), and the Maryland Stem Cell Research Fund (2021-MSCRFD-5697 and 2020-MSCRFD-5372) (L.M.S.R.).

Authorship

Contribution: L.L. and J.-H.K. designed experiments, performed research, interpreted data, and wrote portions of the manuscript; W.L., D.M.W., and J.K. performed experiments and interpreted data; L.C. performed biostatistical analyses and wrote portions of the manuscript; R.K.R. and R.P.K. provided critical reagents and data; L.X. and L.Z.L. performed experiments; M.V. performed Ingenuity Pathway Analysis analyses; D.R.M. provided the GATA2 antibody and helped to edit the manuscript; Z.J.Z. provided JAK-mutant mice; O.R. performed experiments; M.C.S. provided ruxolitinib chow; K.R. provided guidance with ATACseq and chromatin immunoprecipitation experiments; A.-R.R. and B.P. performed scRNAseq analysis of patient samples; J.L.S. provided expertise and reagents and guidance for experiments and helped to write the manuscript; A.R.M. provided expertise and reagents, designed and performed experiments, and helped to write the manuscript; L.M.S.R. conceived the study, designed experiments, reviewed all data, and wrote the manuscript; and all authors reviewed the final manuscript and agreed to be coauthors.

Conflict-of-interest disclosure: M.C.S. is employed by Incyte Research Institute and holds individual shares in this privately held company. R.K.R has received consulting fees from Stemline Therapeutics, Celgene Corporation, Agios Pharmaceuticals, Apex Oncology, Beyond Spring, Partner Therapeutics, and Jazz Pharmaceuticals and has received research funding from Constellation Pharmaceuticals, Incyte Corporation, and Stemline Therapeutics. The remaining authors declare no competing financial interests.

ORCID profiles: L.L., 0000-0002-6884-6059; J.-H.K., 0000-0001-7176-409X; L.Z.L., 0000-0002-8680-4119; D.R.M., 0000-0003-1430-3128; M.C.S., 0000-0003-3771-7083; B.P., 0000-0001-8198-9663; A.R.M., 0000-0002-8673-4317; L.M.S.R., 0000-0002-4004-7060.

Correspondence: Linda M. S. Resar, The Johns Hopkins University School of Medicine, Ross Research Building, Room 1025, 720 Rutland Ave, Baltimore, MD 21205; e-mail: lresar@jhmi.edu.

Footnotes

Submitted 3 September 2021; accepted 18 February 2022; prepublished online on Blood First Edition 14 March 2022. DOI 10.1182/blood.2021013925.

*L.L. and J.-H.K. contributed equally to this study.

DAMI and SET-2 Bulk RNAseq: GSE183374; DAMI ATACseq: GSE189568; DAMI ChIP-seq: GSE 189569; and scRNAseq: GSE197942.

Data sharing requests should be sent to Linda M. S. Resar (lresar@jhmi.edu).

The online version of this article contains a data supplement.

There is a *Blood* Commentary on this article in this issue.

The publication costs of this article were defrayed in part by page charge payment. Therefore, and solely to indicate this fact, this article is hereby marked "advertisement" in accordance with 18 USC section 1734.

REFERENCES

1. Dameshek W. Some speculations on the myeloproliferative syndromes. *Blood*. 1951; 6(4):372-375.
2. Pardanani A, Fridley BL, Lasho TL, Gilliland DG, Tefferi A. Host genetic variation contributes to phenotypic diversity in myeloproliferative disorders. *Blood*. 2008; 111(5):2785-2789.
3. Tam CS, Nussenzveig RM, Popat U, et al. The natural history and treatment outcome of blast phase BCR-ABL- myeloproliferative neoplasms. *Blood*. 2008;112(5):1628-1637.
4. Skoda RC. Hereditary myeloproliferative disorders. *Haematologica*. 2010;95(1):6-8.
5. Lundberg P, Karow A, Nienhold R, et al. Clonal evolution and clinical correlates of somatic mutations in myeloproliferative neoplasms. *Blood*. 2014;123(14):2220-2228.
6. Tefferi A, Guglielmelli P, Larson DR, et al. Long-term survival and blast transformation in molecularly annotated essential thrombocythemia, polycythemia vera, and myelofibrosis. *Blood*. 2014;124(16):2507-2513, quiz 2615.
7. Spivak JL, Considine M, Williams DM, et al. Two clinical phenotypes in polycythemia vera. *N Engl J Med*. 2014; 371(9):808-817.
8. Spivak JL. Myeloproliferative neoplasms. *N Engl J Med*. 2017;376(22):2168-2181.
9. Grinfeld J, Nangalia J, Green AR. Molecular determinants of pathogenesis and clinical phenotype in myeloproliferative neoplasms. *Haematologica*. 2017;102(1):7-17.
10. Tefferi A, Vannucchi AM. Genetic risk assessment in myeloproliferative neoplasms. *Mayo Clin Proc*. 2017;92(8):1283-1290.
11. Marcellino BK, Hoffman R, Tripodi J, et al. Advanced forms of MPNs are accompanied by chromosomal abnormalities that lead to dysregulation of TP53. *Blood Adv*. 2018; 2(24):3581-3589.
12. Schieber M, Crispino JD, Stein B. Myelofibrosis in 2019: moving beyond JAK2 inhibition. *Blood Cancer J*. 2019;9(9):74.
13. Karantanos T, Chaturvedi S, Braunstein EM, et al. Sex determines the presentation and outcomes in MPN and is related to sex-specific differences in the mutational burden. *Blood Adv*. 2020;4(12):2567-2576.
14. Mascarenhas JO, Rampal RK, Kosiorek HE, et al. Phase 2 study of ruxolitinib and decitabine in patients with myeloproliferative neoplasm in accelerated and blast phase. *Blood Adv*. 2020;4(20): 5246-5256.
15. Moliterno AR, Kaizer H. Applied genomics in MPN presentation. *Hematology Am Soc Hematol Educ Program*. 2020;2020(1): 434-439.
16. Moliterno AR, Ginzburg YZ, Hoffman R. Clinical insights into the origins of thrombosis in myeloproliferative neoplasms. *Blood*. 2021;137(9):1145-1153.
17. Grinfeld J, Nangalia J, Baxter EJ, et al. Classification and personalized prognosis in myeloproliferative neoplasms. *N Engl J Med*. 2018;379(15):1416-1430.
18. Van Egeren D, Escabi J, Nguyen M, et al. Reconstructing the lineage histories and differentiation trajectories of individual cancer cells in myeloproliferative neoplasms. *Cell Stem Cell*. 2021;28(3):514-523.e9.
19. Baxter EJ, Scott LM, Campbell PJ, et al; Cancer Genome Project. Acquired mutation of the tyrosine kinase JAK2 in human

Downloaded from http://ashpublications.org/blood/article-pdf/139/18/2797/1895455/bloodbld2021013925.pdf by guest on 29 September 2023

myeloproliferative disorders. *Lancet*. 2005; 365(9464):1054-1061.

20. James C, Ugo V, Le Couédic JP, et al. A unique clonal JAK2 mutation leading to constitutive signalling causes polycythaemia vera. *Nature*. 2005;434(7037):1144-1148.

21. Kralovics R, Passamonti F, Buser AS, et al. A gain-of-function mutation of JAK2 in myeloproliferative disorders. *N Engl J Med*. 2005;352(17):1779-1790.

22. Levine RL, Wadleigh M, Cools J, et al. Activating mutation in the tyrosine kinase JAK2 in polycythemia vera, essential thrombocythemia, and myeloid metaplasia with myelofibrosis. *Cancer Cell*. 2005;7(4): 387-397.

23. Nielsen C, Bojesen SE, Nordestgaard BG, Kofoed KF, Birgens HS. JAK2V617F somatic mutation in the general population: myeloproliferative neoplasm development and progression rate. *Haematologica*. 2014; 99(9):1448-1455.

24. Jaiswal S, Ebert BL. Clonal hematopoiesis in human aging and disease. *Science*. 2019; 366(6465):eaan4673.

25. Pastore F, Bhagwat N, Pastore A, et al. PRMT5 inhibition modulates E2F1 methylation and gene-regulatory networks leading to therapeutic efficacy in $JAK2^{V617F}$-mutant MPN. *Cancer Discov*. 2020;10(11): 1742-1757.

26. Marinaccio C, Suraneni P, Celik H, et al. LKB1/*STK11* is a tumor suppressor in the progression of myeloproliferative neoplasms. *Cancer Discov*. 2021;11(6):1398-1410.

27. Reddy KL, Feinberg AP. Higher order chromatin organization in cancer. *Semin Cancer Biol*. 2013;23(2):109-115.

28. Resar L, Chia L, Xian L. Lessons from the crypt: HMGA1-amping up Wnt for stem cells and tumor progression. *Cancer Res*. 2018; 78(8):1890-1897.

29. Resar LM. The high mobility group A1 gene: transforming inflammatory signals into cancer? *Cancer Res*. 2010;70(2):436-439.

30. Ben-Porath I, Thomson MW, Carey VJ, et al. An embryonic stem cell-like gene expression signature in poorly differentiated aggressive human tumors. *Nat Genet*. 2008;40(5): 499-507.

31. Shah SN, Kerr C, Cope L, et al. HMGA1 reprograms somatic cells into pluripotent stem cells by inducing stem cell transcriptional networks. *PLoS One*. 2012; 7(11):e48533.

32. Chou BK, Mali P, Huang X, et al. Efficient human iPS cell derivation by a non-integrating plasmid from blood cells with unique epigenetic and gene expression signatures. *Cell Res*. 2011;21(3):518-529.

33. Xian L, Georgess D, Huso T, et al. HMGA1 amplifies Wnt signalling and expands the intestinal stem cell compartment and Paneth cell niche. *Nat Commun*. 2017;8(1):15008.

34. Reeves R, Beckerbauer L. HMGI/Y proteins: flexible regulators of transcription and chromatin structure. *Biochim Biophys Acta*. 2001;1519(1-2):13-29.

35. Pomeroy SL, Tamayo P, Gaasenbeek M, et al. Prediction of central nervous system embryonal tumour outcome based on gene expression. *Nature*. 2002;415(6870):436-442.

36. Sarhadi VK, Wikman H, Salmenkivi K, et al. Increased expression of high mobility group A proteins in lung cancer. *J Pathol*. 2006; 209(2):206-212.

37. Tesfaye A, Di Cello F, Hillion J, et al. The high-mobility group A1 gene up-regulates cyclooxygenase 2 expression in uterine tumorigenesis. *Cancer Res*. 2007;67(9): 3998-4004.

38. Hillion J, Wood LJ, Mukherjee M, et al. Upregulation of MMP-2 by HMGA1 promotes transformation in undifferentiated, large-cell lung cancer. *Mol Cancer Res*. 2009;7(11):1803-1812.

39. Hristov AC, Cope L, Di Cello F, et al. HMGA1 correlates with advanced tumor grade and decreased survival in pancreatic ductal adenocarcinoma. *Mod Pathol*. 2010; 23(1):98-104.

40. Hillion J, Smail SS, Di Cello F, et al. The HMGA1-COX-2 axis: a key molecular pathway and potential target in pancreatic adenocarcinoma. *Pancreatology*. 2012;12(4): 372-379.

41. Shah SN, Cope L, Poh W, et al. HMGA1: a master regulator of tumor progression in triple-negative breast cancer cells. *PLoS One*. 2013;8(5):e63419.

42. Belton A, Gabrovsky A, Bae YK, et al. HMGA1 induces intestinal polyposis in transgenic mice and drives tumor progression and stem cell properties in colon cancer cells. *PLoS One*. 2012;7(1): e30034.

43. Hillion J, Roy S, Heydarian M, et al. The high mobility group A1 (HMGA1) gene is highly overexpressed in human uterine serous carcinomas and carcinosarcomas and drives matrix metalloproteinase-2 (MMP-2) in a subset of tumors. *Gynecol Oncol*. 2016;141(3): 580-587.

44. Gorbounov M, Carleton NM, Asch-Kendrick RJ, et al. High mobility group A1 (HMGA1) protein and gene expression correlate with ER-negativity and poor outcomes in breast cancer. *Breast Cancer Res Treat*. 2020; 179(1):25-35.

45. Thanos D, Maniatis T. The high mobility group protein HMG I(Y) is required for NF-kappa B-dependent virus induction of the human IFN-beta gene. *Cell*. 1992;71(5): 777-789.

46. Zhao K, Käs E, Gonzalez E, Laemmli UK. SAR-dependent mobilization of histone H1 by HMG-I/Y in vitro: HMG-I/Y is enriched in H1-depleted chromatin. *EMBO J*. 1993; 12(8):3237-3247.

47. Saitoh Y, Laemmli UK. Metaphase chromosome structure: bands arise from a differential folding path of the highly AT-rich scaffold. *Cell*. 1994;76(4):609-622.

48. Geierstanger BH, Volkman BF, Kremer W, Wemmer DE. Short peptide fragments derived from HMG-I/Y proteins bind specifically to the minor groove of DNA. *Biochemistry*. 1994;33(17):5347-5355.

49. Thanos D, Maniatis T. Virus induction of human IFN beta gene expression requires the assembly of an enhanceosome. *Cell*. 1995;83(7):1091-1100.

50. Falvo JV, Thanos D, Maniatis T. Reversal of intrinsic DNA bends in the IFN beta gene enhancer by transcription factors and the architectural protein HMG I(Y). *Cell*. 1995; 83(7):1101-1111.

51. Maher JF, Nathans D. Multivalent DNA-binding properties of the HMG-1 proteins. *Proc Natl Acad Sci USA*. 1996;93(13): 6716-6720.

52. Huth JR, Bewley CA, Nissen MS, et al. The solution structure of an HMG-I(Y)-DNA complex defines a new architectural minor groove binding motif. *Nat Struct Biol*. 1997; 4(8):657-665.

53. Hillion J, Dhara S, Sumter TF, et al. The high-mobility group A1a/signal transducer and activator of transcription-3 axis: an Achilles heel for hematopoietic malignancies? *Cancer Res*. 2008;68(24):10121-10127.

54. Schuldenfrei A, Belton A, Kowalski J, et al. HMGA1 drives stem cell, inflammatory pathway, and cell cycle progression genes during lymphoid tumorigenesis. *BMC Genomics*. 2011;12(1):549.

55. Xu Y, Sumter TF, Bhattacharya R, et al. The HMG-I oncogene causes highly penetrant, aggressive lymphoid malignancy in transgenic mice and is overexpressed in human leukemia. *Cancer Res*. 2004;64(10): 3371-3375.

56. Di Cello F, Dhara S, Hristov AC, et al. Inactivation of the Cdkn2a locus cooperates with HMGA1 to drive T-cell leukemogenesis. *Leuk Lymphoma*. 2013;54(8):1762-1768.

57. Roy S, Di Cello F, Kowalski J, et al. HMGA1 overexpression correlates with relapse in childhood B-lineage acute lymphoblastic leukemia. *Leuk Lymphoma*. 2013;54(11): 2565-2567.

58. Wood LJ, Mukherjee M, Dolde CE, et al. HMG-I/Y, a new c-Myc target gene and potential oncogene. *Mol Cell Biol*. 2000; 20(15):5490-5502.

59. Wood LJ, Maher JF, Bunton TE, Resar LM. The oncogenic properties of the HMG-I gene family. *Cancer Res*. 2000;60(15): 4256-4261.

60. Nelson DM, Joseph B, Hillion J, Segal J, Karp JE, Resar LM. Flavopiridol induces BCL-2 expression and represses oncogenic transcription factors in leukemic blasts from adults with refractory acute myeloid leukemia. *Leuk Lymphoma*. 2011;52(10): 1999-2006.

61. Karp JE, Smith BD, Resar LS, et al. Phase 1 and pharmacokinetic study of bolus-infusion flavopiridol followed by cytosine arabinoside and mitoxantrone for acute leukemias. *Blood*. 2011;117(12):3302-3310.

Downloaded from http://ashpublications.org/blood/article-pdf/139/18/2797/1895455/bloodbld2021013925.pdf by guest on 29 September 2023

62. Bao EL, Nandakumar SK, Liao X, et al; 23andMe Research Team. Inherited myeloproliferative neoplasm risk affects haematopoietic stem cells. *Nature*. 2020; 586(7831):769-775.

63. Skarnes WC, Rosen B, West AP, et al. A conditional knockout resource for the genome-wide study of mouse gene function. *Nature*. 2011;474(7351):337-342.

64. Xing S, Wanting TH, Zhao W, et al. Transgenic expression of JAK2V617F causes myeloproliferative disorders in mice. *Blood*. 2008;111(10):5109-5117.

65. Spivak JL, Merchant A, Williams DM, et al. Thrombopoietin is required for full phenotype expression in a JAK2V617F transgenic mouse model of polycythemia vera. *PLoS One*. 2020;15(6):e0232801.

66. Mayle A, Luo M, Jeong M, Goodell MA. Flow cytometry analysis of murine hematopoietic stem cells. *Cytometry A*. 2013;83(1):27-37.

67. Freitas C, Wittner M, Nguyen J, et al. Lymphoid differentiation of hematopoietic stem cells requires efficient Cxcr4 desensitization. *J Exp Med*. 2017;214(7): 2023-2040.

68. Gudmundsson KO, Nguyen N, Oakley K, et al. *Prdm16* is a critical regulator of adult long-term hematopoietic stem cell quiescence. *Proc Natl Acad Sci USA*. 2020; 117(50):31945-31953.

69. Buenrostro JD, Giresi PG, Zaba LC, Chang HY, Greenleaf WJ. Transposition of native chromatin for fast and sensitive epigenomic profiling of open chromatin, DNA-binding proteins and nucleosome position. *Nat Methods*. 2013;10(12):1213-1218.

70. Psaila B, Wang G, Rodriguez-Meira A, et al; NIH Intramural Sequencing Center. Single-cell analyses reveal megakaryocyte-biased hematopoiesis in myelofibrosis and identify mutant clone-specific targets. *Mol Cell*. 2020;78(3):477-492.e8.

71. Rodriguez-Meira A, Buck G, Clark SA, et al. Unravelling intratumoral heterogeneity through high-sensitivity single-cell mutational analysis and parallel RNA sequencing. *Mol Cell*. 2019;73(6):1292-1305.e8.

72. Dingler FA, Wang M, Mu A, et al. Two aldehyde clearance systems are essential to prevent lethal formaldehyde accumulation in mice and humans. *Mol Cell*. 2020;80(6): 996-1012.e9.

73. Greenberg SM, Rosenthal DS, Greeley TA, Tantravahi R, Handin RI. Characterization of a new megakaryocytic cell line: the Dami cell. *Blood*. 1988;72(6):1968-1977.

74. MacLeod RA, Dirks WG, Reid YA, Hay RJ, Drexler HG. Identity of original and late passage Dami megakaryocytes with HEL erythroleukemia cells shown by combined cytogenetics and DNA fingerprinting. *Leukemia*. 1997;11(12):2032-2038.

75. Quentmeier H, MacLeod RA, Zaborski M, Drexler HG. JAK2 V617F tyrosine kinase mutation in cell lines derived from myeloproliferative disorders. *Leukemia*. 2006;20(3):471-476.

76. Fiedler W, Henke RP, Ergün S, et al. Derivation of a new hematopoietic cell line with endothelial features from a patient with transformed myeloproliferative syndrome: a case report. *Cancer*. 2000;88(2):344-351.

77. Subramanian A, Tamayo P, Mootha VK, et al. Gene set enrichment analysis: a knowledge-based approach for interpreting genome-wide expression profiles. *Proc Natl Acad Sci USA*. 2005;102(43):15545-15550.

78. Liberzon A, Birger C, Thorvaldsdóttir H, Ghandi M, Mesirov JP, Tamayo P. The Molecular Signatures Database (MSigDB) hallmark gene set collection. *Cell Syst*. 2015; 1(6):417-425.

79. Zini R, Guglielmelli P, Pietra D, et al; AGIMM (AIRC Gruppo Italiano Malattie Mieloproliferative) investigators. CALR mutational status identifies different disease subtypes of essential thrombocythemia showing distinct expression profiles. *Blood Cancer J*. 2017;7(12):638.

80. Paul F, Arkin Y, Giladi A, et al. Transcriptional heterogeneity and lineage commitment in myeloid progenitors [published correction appears in *Cell*. 2016;164(1-2):325]. *Cell*. 2015;163(7): 1663-1677.

81. Giladi A, Paul F, Herzog Y, et al. Single-cell characterization of haematopoietic progenitors and their trajectories in homeostasis and perturbed haematopoiesis. *Nat Cell Biol*. 2018;20(7):836-846.

82. Nam AS, Kim KT, Chaligne R, et al. Somatic mutations and cell identity linked by genotyping of transcriptomes. *Nature*. 2019; 571(7765):355-360.

83. Izzo F, Lee SC, Poran A, et al. DNA methylation disruption reshapes the hematopoietic differentiation landscape. *Nat Genet*. 2020;52(4):378-387.

84. Tsai FY, Keller G, Kuo FC, et al. An early haematopoietic defect in mice lacking the transcription factor GATA-2. *Nature*. 1994; 371(6494):221-226.

85. Bresnick EH, Jung MM, Katsumura KR. Human GATA2 mutations and hematologic disease: how many paths to pathogenesis? *Blood Adv*. 2020;4(18):4584-4592.

86. Huang Z, Dore LC, Li Z, et al. GATA-2 reinforces megakaryocyte development in the absence of GATA-1. *Mol Cell Biol*. 2009; 29(18):5168-5180.

87. Menendez-Gonzalez JB, Sinnadurai S, Gibbs A, et al. Inhibition of GATA2 restrains cell proliferation and enhances apoptosis and chemotherapy mediated apoptosis in human GATA2 overexpressing AML cells. *Sci Rep*. 2019;9(1):12212.

88. Akada H, Yan D, Zou H, Fiering S, Hutchison RE, Mohi MG. Conditional expression of heterozygous or homozygous Jak2V617F from its endogenous promoter induces a polycythemia vera-like disease. *Blood*. 2010; 115(17):3589-3597.

89. Iacobucci I, Li Y, Roberts KG, et al. Truncating erythropoietin receptor rearrangements in acute lymphoblastic leukemia. *Cancer Cell*. 2016;29(2):186-200.

90. Maude SL, Tasian SK, Vincent T, et al. Targeting JAK1/2 and mTOR in murine xenograft models of Ph-like acute lymphoblastic leukemia. *Blood*. 2012;120(17): 3510-3518.

91. Gilles L, Arslan AD, Marinaccio C, et al. Downregulation of GATA1 drives impaired hematopoiesis in primary myelofibrosis. *J Clin Invest*. 2017;127(4):1316-1320.

92. Zingariello M, Sancillo L, Martelli F, et al. The thrombopoietin/MPL axis is activated in the Gata1^{low} mouse model of myelofibrosis and is associated with a defective RPS14 signature. *Blood Cancer J*. 2017;7(6):e572.

93. Vannucchi AM, Pancrazzi A, Guglielmelli P, et al. Abnormalities of GATA-1 in megakaryocytes from patients with idiopathic myelofibrosis. *Am J Pathol*. 2005;167(3):849-858.

94. Kleppe M, Koche R, Zou L, et al. Dual targeting of oncogenic activation and inflammatory signaling increases therapeutic efficacy in myeloproliferative neoplasms [published correction appears in *Cancer Cell*. 2018;33(4):785–787]. *Cancer Cell*. 2018;33(1):29-43.e7.

95. Ikeda K, Mason PJ, Bessler M. 3′UTR-truncated Hmga2 cDNA causes MPN-like hematopoiesis by conferring a clonal growth advantage at the level of HSC in mice. *Blood*. 2011;117(22):5860-5869.

96. Dutta A, Hutchison RE, Mohi G. Hmga2 promotes the development of myelofibrosis in Jak2^{V617F} knockin mice by enhancing TGF-β1 and Cxcl12 pathways. *Blood*. 2017; 130(7):920-932.

97. Ueda K, Ikeda K, Ikezoe T, et al. Hmga2 collaborates with *JAK2*V617F in the development of myeloproliferative neoplasms. *Blood Adv*. 2017;1(15): 1001-1015.

98. Marquis M, Beaubois C, Lavallée VP, et al. High expression of HMGA2 independently predicts poor clinical outcomes in acute myeloid leukemia [published correction appears in *Blood Cancer J*. 2019;9(3):28]. *Blood Cancer J*. 2018;8(8):68.

© 2022 by The American Society of Hematology

Downloaded from http://ashpublications.org/blood/article-pdf/139/18/2797/1895455/bloodbld2021013925.pdf by guest on 29 September 2023